Department of Structural Engineering
Faculty of Engineering Science and Technology
NTNU- Norwegian University of Science and Technology

ACCESSIBILITY

OPEN

MASTER THESIS 2010

SUBJECT AREA:	DATE:	NO. OF PAGES:
FE-analysis, dynamics	14.06.2010	71+23

TITLE:

Static and dynamic response of a structure subjected to ice forces – Evaluation of a lighthouse overloading event

Statisk og dynamisk respons av en konstruksjon utsatt for islaster- Evaluering av overbelastningen av et fyrtårn

BY:

Vegard Sætre Bjoland

SUMMARY:
Exploitation of areas and natural resources in arctic and sub-arctic areas makes guidelines for designing structures exposed to ice-forces a necessity. Ice actions on a structure include both static and dynamic components, and methods to calculate the magnitude of the ice loads are given in several common design codes. The static load component is constant and dependent on structure geometry and ice thickness, while dynamic loading is given in the design codes as time varying forcing functions.

In the winter of 1985 Björnklacken lighthouse, located north in the Bothnian Bay, was overloaded by ice forces and displaced along the seabed. A numerical model has been created using the FEA software package ABAQUS to determine the static response and the structural properties of Björnklacken. The structural properties have further been used in the analysis of a single degree of freedom (SDOF)-system to determine dynamic response.

The static and dynamic ice load components given by common design codes have been applied to both the numerical model and the SDOF-system. Initial calculations revealed large differences between the predicted loads from the different codes. Dynamic analysis showed that the response caused by a harmonic forcing function was significantly higher than that which was caused by a sawtooth forcing function.

Results also showed that the amplitude of the dynamic forcing function is reduced if the structure's velocity at loading point is scaled as a ratio of the ice velocity. The reduction is more severe with lower damping, resulting in higher reductions in systems with low damping fractions. Given the close relation between velocity at waterline and dynamic response, a recommendation is that guidelines for velocity scaling should be included in all of the design codes.

RESPONSIBLE TEACHER: Prof. Kjell Magne Mathisen, NTNU

SUPERVISOR(S): Morten Bjerkås, Phd., Specialist Engineer, Reinertsen AS

CARRIED OUT AT: NTNU, Trondheim

MASTER THESIS
SPRING TERM 2010

Prediction of the response from ice forces on a lighthouse structure

Background
An offshore lighthouse structure "Björnklacken" located on the Swedish coastline in the Gulf of Bothnia has failed due to excessive ice loading (Figure 1). Few details have been quantified to figure out the reasons for overloading.

The aim of the present project is to develop a FE model of the lighthouse to back calculate the level of ice forces that caused failure of the structure. The load levels should be compared to modern design requirements for ice actions against offshore structures. Key literature is listed in the reference list.

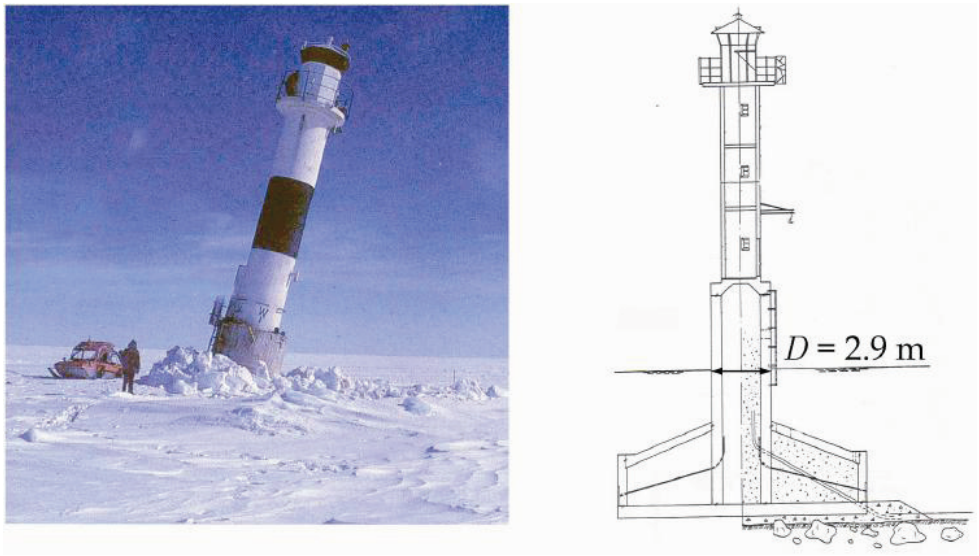

Figure 1. Tower of Björnklacken lighthouse broken winter 1969/1970 (Bjerkås, 2006).

Scope of work
Scope of work is divided in three parts:

- Numerical modelling of an offshore lighthouse structure with FE software ABAQUS
- Quantification of the magnitude of static and dynamic structural response
- Comparison of the most common design codes for ice load prediction

1) Numerical modelling
The candidate will get structural drawings from Reinertsen AS to be used as the basis for geometrical modelling. The concrete walls could preferably be modelled with shell elements. Clear figures showing the geometry and dimensions of the structure

should be presented. A list of nodes and element types should also be presented. An input file should be printed in appendix of the thesis.

2) Structural response analyses
Static and dynamic response of the lighthouse should be presented. Eigenfrequencies should be tuned with adjusting total mass, stiffness and boundary conditions. Main steps in analyses are:

- Present the 10 first eigenmodes of the structure
- Present load vs structural inclination at different levels in the structure (levels given in drawings)

Reporting
A time schedule should be presented in written form at the second project meeting. The thesis should be presented in written form, common rules of reporting technical work should be met. The thesis should be presented orally at Reinertsen AS main office.

References
Bjerkås, M., (2006), Ice actions on offshore structures, PhD Thesis, Norwegian University of Science and Technology, June 2006.

http://www.vindenergi.org/Vindforskrapporter/09_55_report.pdf

http://cvi.se/uploads/pdf/Kunskapsdatabas%20teknik/forskningsresultat/CTH_Bergdahl_Israpport.pdf

Responsible at NTNU: Prof. Kjell Magne Mathisen

Supervisor at Reinertsen AS: Morten Bjerkås, PhD

The thesis should be given NTNU before: 15.06.10

Trondheim 18.01.10

Signed by responsible: _____

Preface

This thesis is the product of a well spent spring semester at the Norwegian University of Science and Technology in Trondheim, Norway. The assignment was given by Reinertsen AS and was written as a part of my Master of Science degree in Structural Engineering in the spring 2010.

My gratitude goes to my supervisor Morten Bjerkås, specialist engineer at Reinertsen AS, for his worthy advice and inspiring guidance. I would also like to thank Dr. Lennart Fransson at the University of Luleå for providing me with a report critical to my work on Björnklacken.

Thanks also go to Tor Øyvind Lehmann for good cooperation and Frode Seglem and Runar Heggen for their good company at the office during the semester.

Vegard Sætre Bjoland
Trondheim, 14.Juni 2010

Contents

List of Figures

List of Tables

Symbols and Abbreviations

f	Frequency
h_i	Ice thickness
h_s	Snow depth
k_i	Mean thermal conductivity of ice
k_s	Mean thermal conductivity of snow
l_f	Latent heat fusion of ice
p_G	Ice pressure
q	Amplitude fraction
u	Structural displacement at loading point
$\dot{u}$	Structural velocity at loading point
$\ddot{u}$	Structural acceleration at loading point
v_t	Ice velocity
C_n	Damping factor
C_R	Ice strength coefficient (ISO)
D	Diameter of structure
F_D	Design load
F_{dyn}	Dynamic ice load
F_f	Frictional force
F_G	Static ice load
F_{OT}	Overturning load
G	Weight
K_n	Modal stiffness
M_n^*	Generalised mass

M_n	Modal mass
M_D	Design moment
T_a	Mean ambient air temperature
T_m	Melting point temperature of ice
ω	Angular frequency
α	Shape factor (Kärnä)
$\gamma(\alpha)$	Correction factor (Kärnä)
ϕ	Modal amplitude
ρ_i	Density of solid ice
σ	Ice crushing strength (IEC)
θ	Stability coefficient
μ	Coefficient of friction
ξ	Damping ratio
ξ_{crit}	Critical damping ratio
API	American Petroleum Institute
DAF	Dynamic Amplification Factor
FDD	Freezing-degree-days
FE	Finite Element
IEC	International Electrotechnical Commision
ISO	International Organization for Standardization
SDOF	Single degree of freedom
SMHI	Sveriges meteorologiska och hydrologiska institut
WL	Waterline

1 Introduction

1.1 General

Abundant natural resources and large unused areas encourages expansion in arctic and sub-arctic areas, in spite of harsh conditions. In year 2000, the U.S. Geological Survey World Assessment Team made an estimate of the total mean undiscovered oil and gas resources within the Arctic Circle. They estimated that there was approximately 90 billion barrels of oil, 47 trillion cubic metres of natural gas and 44 billion barrels of natural gas liquids still not discovered (USGS 2000). Exploitation of resources in sub-arctic and arctic areas makes accurate guidelines for predicting the response of constructions exposed to extreme ice-loads necessary. Plans also exists for the developement of large wind farms in the Baltic Sea, and these plans require similar guidelines. Several design codes contain methods of calculation to predict ice loads, but the accuracy of these methods are uncertain.

The JZ20-2 MUQ & MNW platform, located in the Bohai Bay in China, is shown in Figure 1.1. Problems with dynamic ice response are common in the area, and a report by Yue and Bi (2001) has revealed the JZ20-2 platform's sensitivity to vibrations.

Similar problems has also been reported for the Lunskoye-A platform, shown in Figure 1.2. The platform lies in the Sakhalin-II field near Sakhalin Island, off the east coast of Russia, and experienced vibrations caused by ice action already in its first year of operation (Kärnä et. al. 2007).

The Molikpaq platform, shown in Figure 1.3, has operated on several sites in the Beaufort Sea. In spite of its wide base, the Molikpaq platform have experienced vibrations caused by ice actions. Several studies have been carried out to analyse data on interaction between ice and structures (Bjerkaas 2006).

Figure 1.1: JZ20-2 MUQ & MNW platform (Kärnä et. al. 2006)

Figure 1.2: The Lunskoye-A platform in the Sakhalin II field (photo: Shell)

Figure 1.3: The Molikpaq platform in the Beaufort Sea (photo: Shell)

1.2 Ice loads

In sub-arctic areas, such as the Bothnian Bay, the sea is often covered in ice a large portion of the year. This makes first-year ice features, which include level ice, rafted ice, ice floes etc. a common problem. Ice action on vertical structures consists of both static and dynamic force components. Static ice loads are often due to level ice continuously crushing against the structure. Calculation of static loads are made without regards to vibrations caused by ice-structure interaction, and are dependent on factors such as the crushing strength of ice, ice thickness and the dimensions of the structure.

Dynamic ice action includes ductile crushing, intermittent crushing and continuous crushing, illustrated in Figure 1.4. When the ice acts with moderate speed on a structure, self-excited vibrations may occur. Self-excited vibration, also known as frequency lock-in, leads to steady-state vibrations in the structure. If a structure proves to be susceptible to self-excited vibrations, dynamic analysis has to be carried out. Through dynamic analysis, the dynamic amplification of the ice load can be determined.

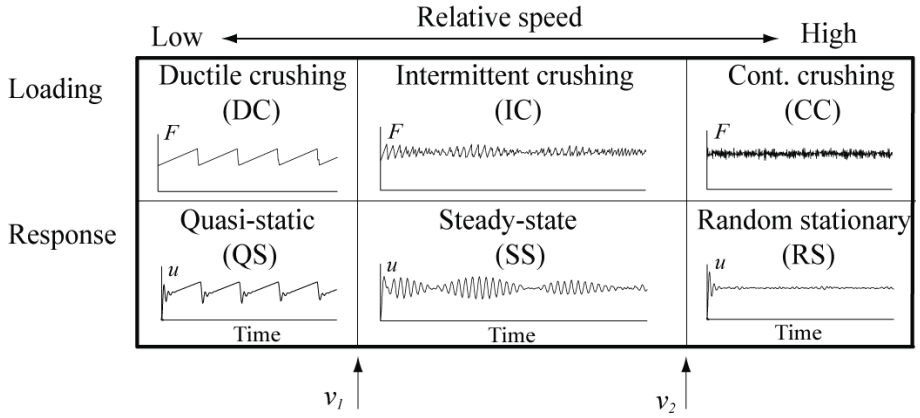

Figure 1.4: Types of dynamic ice-structure interactions (Bjerkås 2006)

Different design codes provides different methods for applying dynamic ice action in an analysis. Two forcing functions will be used for the purpose of dynamic analysis in this report: A sawtooth forcing function and a harmonic forcing function. Closer description of these forcing functions is given in Chapter 3.

1.3 Scope of work

The scope of the present work includes the following main objectives:

- Make a numerical model of Björnklacken lighthouse using the finite element software package ABAQUS
- Perform modal analysis to determine the fundamental modes and the related modal properties for the structure
- Determine static and dynamic force components in accordance with the most commonly used design codes
- Evaluate the magnitude of the predicted ice action calculated in accordance with the design codes and compare the results

2 Background

2.1 Björnklacken Lighthouse

Björnklacken and its twin lighthouse, Borussiaground, were installed in 1969. The twin lighthouses were installed of the coast of Sweden, far north in the Gulf Of Bothnia, to serve as guidance along two fairways leading to the Luleå Harbour (Engelbrektson 1987). Their location is shown in Figure 2.1 and 2.2. In this area the sea is covered by ice for as much as 100-150 days per year (Kullenberg 1981).

Both Björnklacken and Borussiaground were constructed as pure gravity base structures. Björnklacken was approximately 20.9 m tall, and stood at approximately 7 m deep water. A sketch of the lighthouse is shown in Figure 2.3. Due to the availability and price of iron ore at the time, the lighthouses' bases were filled with iron ore (Engelbrektsson 1987). During their first winter of operation, both lighthouses were reported to shift along the seabed, indicating that the ice forces acting on them had been underestimated. Björnklacken was reported to have shifted 10 cm and Borussiaground some cm (Björk 1981).

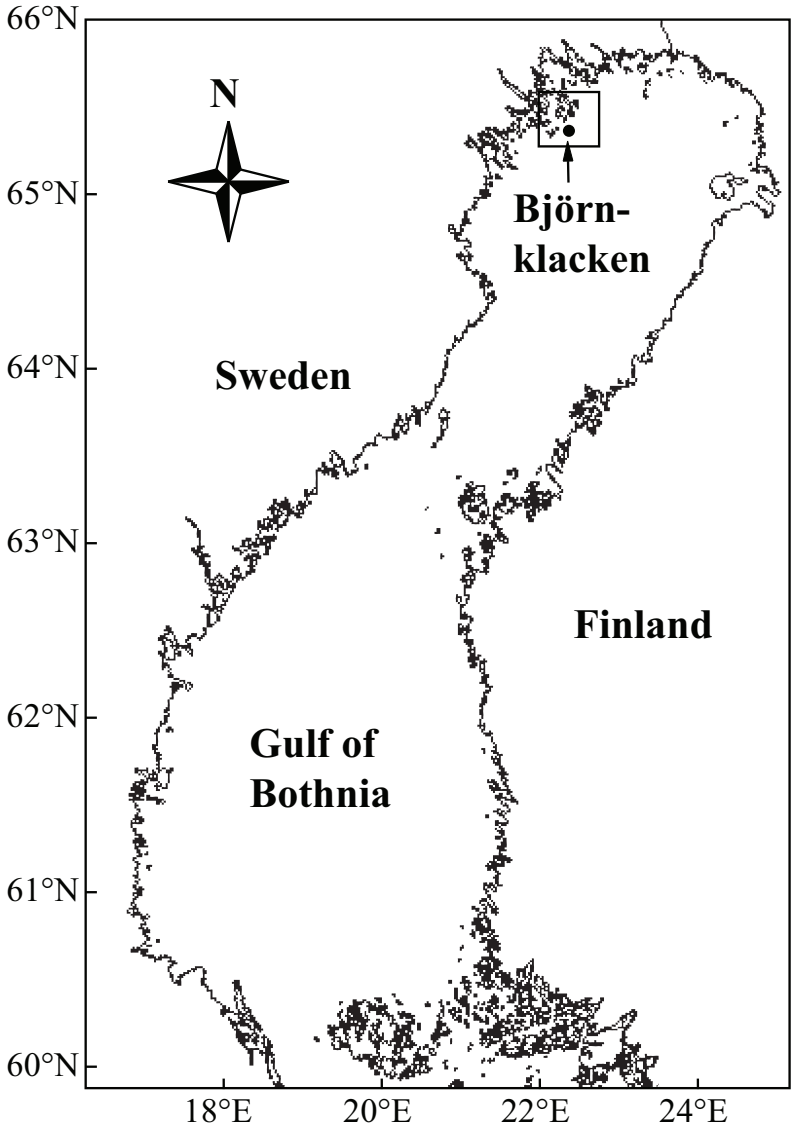

Figure 2.1: Map showing the location of Björnklacken Lighthouse

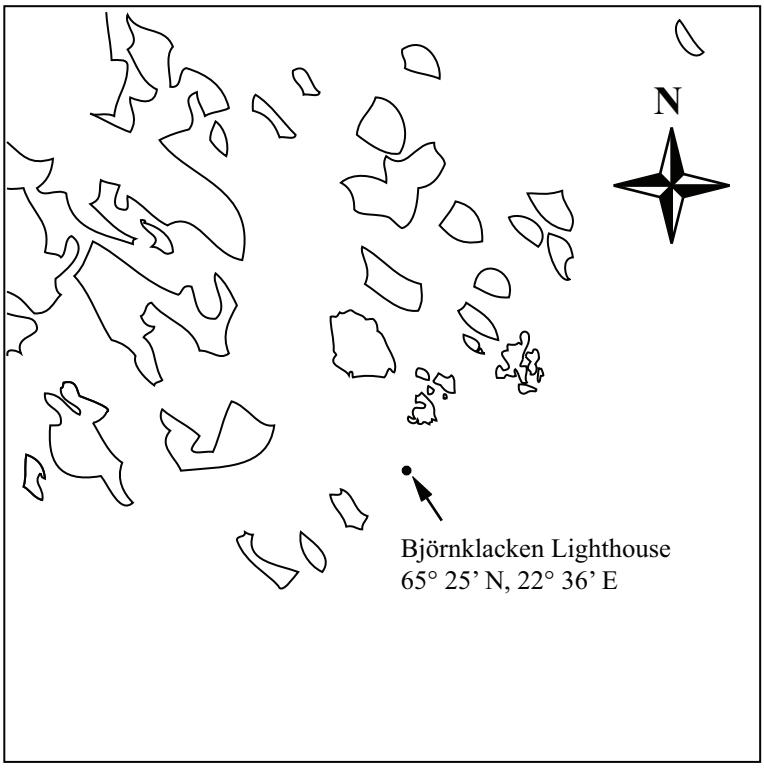

Figure 2.2: Detailed map of the location of Björnklacken

To prevent further displacement, the lighthouses were equipped with pre-stressed post-tensioned rock anchors. The rock anchors were drilled into bore holes below the centre tower, shown in Figure 2.3. Each of the rock anchors consisted of seven 0.5" strands, and were post-tensioned up to about 70% of the ultimate tensile strength (Engelbrektsson 1987).

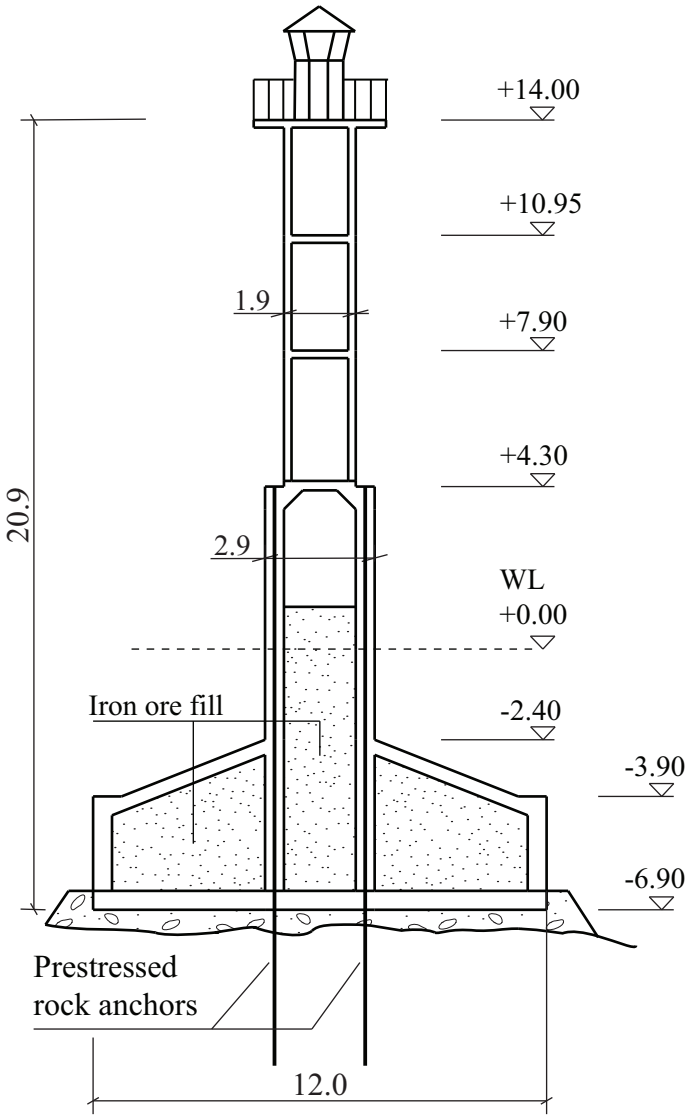

Figure 2.3: Björnklacken with dimensions

On the 4th of April 1985, Björnklacken was overloaded and the rock anchors broke. The lighthouse was moved 17 meters from its bed by ice forces, and came to rest on a seabed incline, shown in Figure 2.4. The winter the failure occured was very cold, with high ice growth and large ice forces. Maximum ice thickness in the winter of 1984/85 was approximately 0.91 meters, while the mean ice thickness for the period 1965-1995 was approximately 0.79 m. An overview of yearly ice growth is shown in Figure 4.2.

High ice growth combined with strong, homogenous ice, severe wind speeds and the appearance of a large ice floe was believed to be the cause of Björnklacken's failure (Engelbrektsson 1987).

Björnklacken's resting position after failure is shown in Figure 2.4. In Figure 2.5, ice has piled up against the lighthouse tower, causing a local increase in ice thickness. Figure 2.6 shows how the drift ice has broken around the structure.

Figure 2.4: Björnklacken, after failure in 1985 (Engelbrektson 1987)

Figure 2.5: Björnklacken lighthouse, view from NW (Engelbrektson 1987)

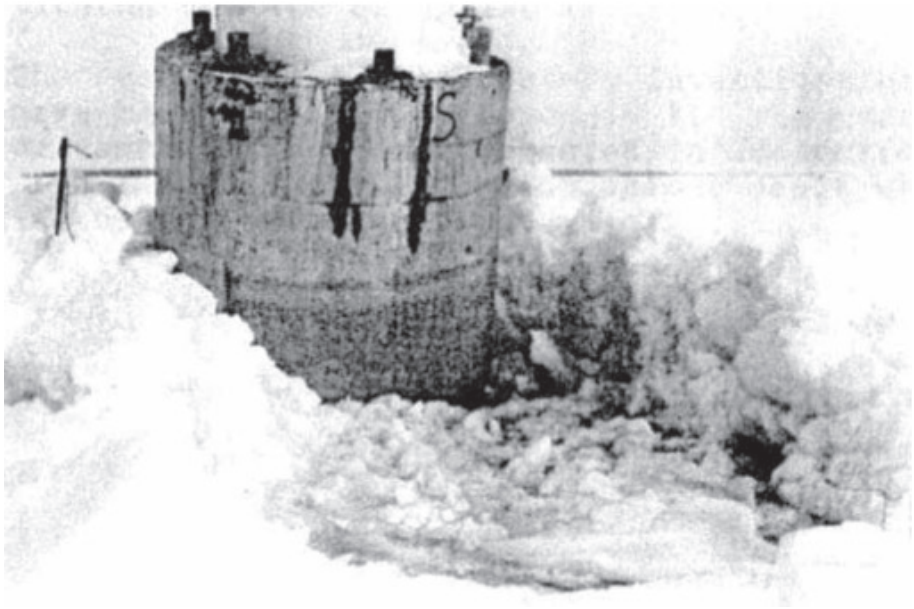

Figure 2.6: Björnklacken ligthouse, view from SW (Engelbrektson 1987)

In Figure 2.7 a timeline showing the main events in Björnklackens lifetime is presented. While in operation, no other incidents than the displacement in 1970 and the failure in 1985 occured.

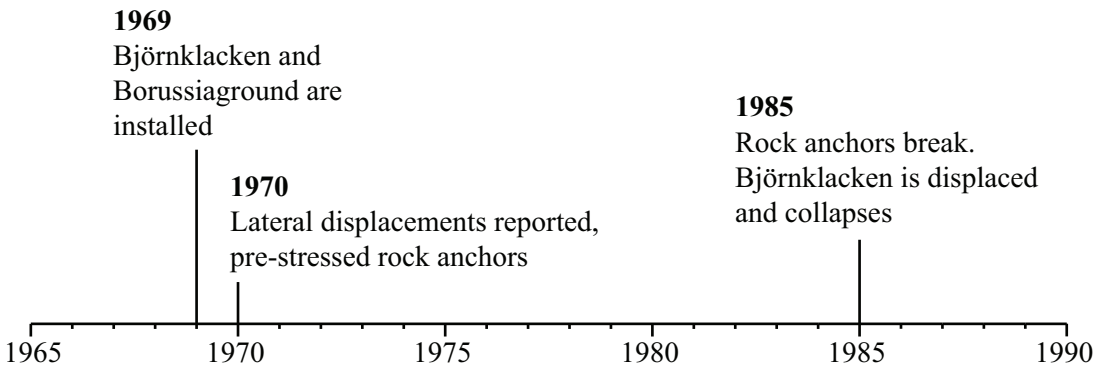

Figure 2.7: The lifetime of Björnklacken

2.2 Previous work

In 1985, shortly after the overloading of Björnklacken, Fransson at the University of Luleå and Engelbrektsson from VBB carried out a study project in which they investigated the event (Engelbrektson 1987).

Based on numerical assumptions and observations from the site of failure, Engelbrektsson et. al. argued that the failure had happened due to extreme ice forces that winter. The extreme ice forces was a result of a combination of several factors. These included strong homogenous ice, extremely thick ice around the lighthouse and rapid ice movement (Engelbrektsson 1987).

Engelbrektsson reported that ice, with a thickness as high as 1.4 - 1.5 meters, had been surrounding the lighthouse when the site had been inspected after failure. The rapid ice movement was mainly due to high wind speeds, but was not included in any calculations in Engelbrektsson's report. It can be assumed that rapid ice movements were mentioned as an indicator that dynamic effects may have occured. A large ice floe was also mentioned in Engelbrektsson's work as a contributing cause for the failure. Detailed calculations describing it's influence, however, was not included in their work.

Failure was assumed to have started with the tearing-off of the rock anchors caused by an overturning moment. The ultimate overturning moment that Björnklacken could sustain was calculated to be 10.9 MN, based on a weight of 8.7 MN and the four pre-stressed rock anchors.

Figure 2.8 shows Björnklackens position before and after the failure. The inclined position

which can be observed i.a. in Figure 2.4, was due to the slope of the seabed at Björnklackens resting position.

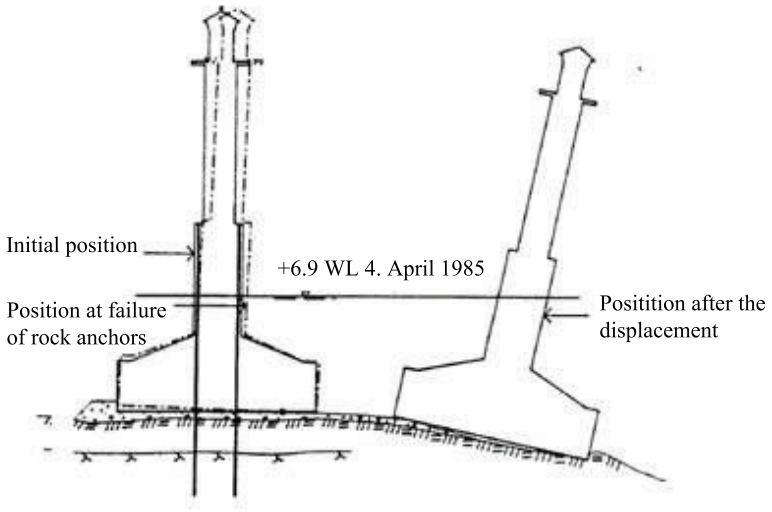

Figure 2.8: Björnklacken in inclined position (Engelbrektsson 1987)

Ice loads have been the documented cause of failure for several other structures in arctic areas. Nygrån lighthouse collapsed during the winter 1968/69 and the Vallinsgrund lighthouse collapsed in April 1979. Both lighthouses were located in the Bothnian Bay and both failed as a redult of excessive ice forces (Björk 1981). A study is currently being performed by Lehmann (2010) as his master thesis, studying the cause of Nygrån lighthouse's collapse.

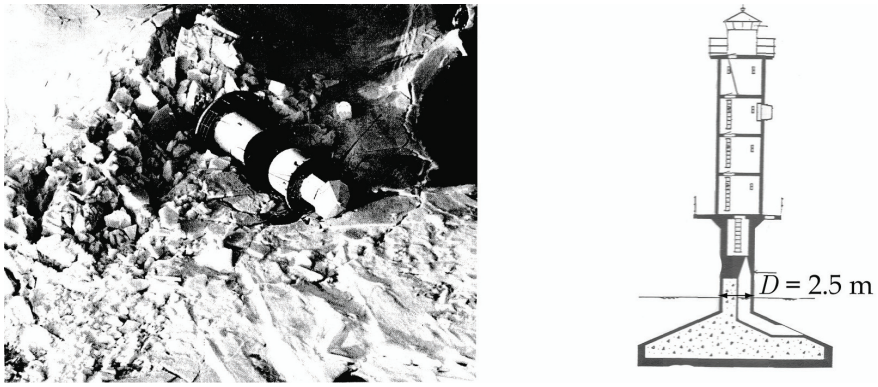

Figure 2.9: Nygrån lighthouse, collapsed in the winter 1968/69 (Bjerkaas 2006)

3 Method

3.1 Ice Growth

Sea ice growth is mainly driven by air temperature and, to a varying extent, the thickness of existing ice, snow thickness and wind. Air temperature measured at Luleå airport (SMHI 2010), approximately 57 km from Björnklacken, is shown in Figure 3.1.

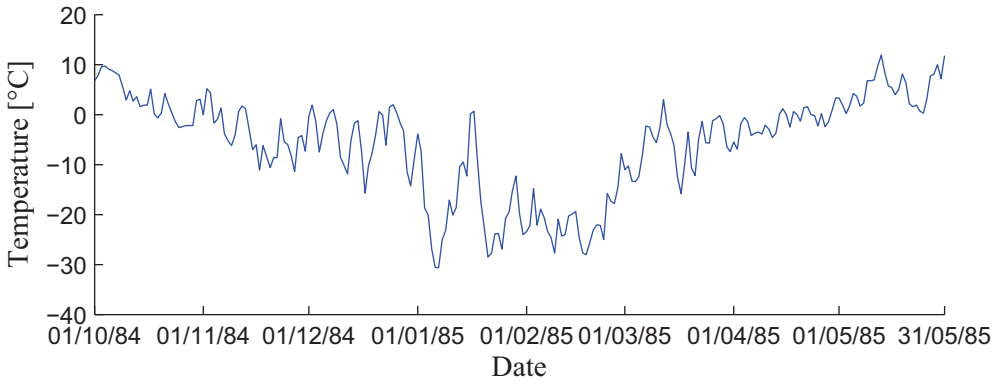

Figure 3.1: Air temperature at Luleå Airport in the winter 84/85 (SMHI 1985)

Both analytical and empirical equations for the calculation of ice thickness exists. Stefan-Boltzmann law, also known as Stefan's law of radiation, can be used for the this purpose, and is given by:

$$h_i^2 = \frac{2k_i}{l_f \rho_i} \int_0^t (T_m - T_a)dt = \frac{2k_i}{l_f \rho_i} FDD \tag{3.1}$$

where h_i is the ice thickness, k_i is the mean thermal conductivity of ice, l_f is the latent heat of fusion of ice, and ρ_i is the density of solid ice. T_m and T_a are the melting point temperature of ice and the mean ambient air temperature and FDD is freezing-degree-days, temperature of freezing

days integrated over time. Figure 3.2 shows FDD for each winter in the time period 1965-1995, calculated based on the data from SMHI.

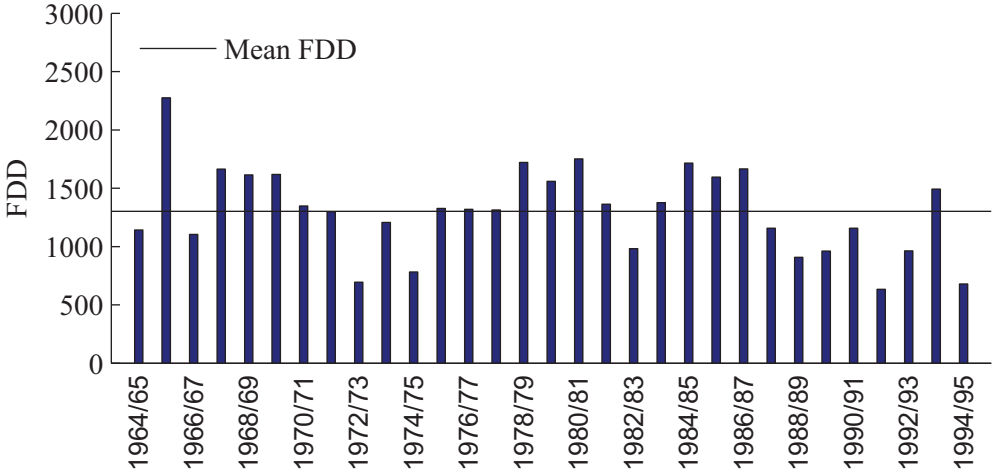

Figure 3.2: FDD for the period 1965-1995

Recordings of the snow depth at Luleå Airport, which is the nearest place where recordings have been carried out, are shown in Figure 3.3.

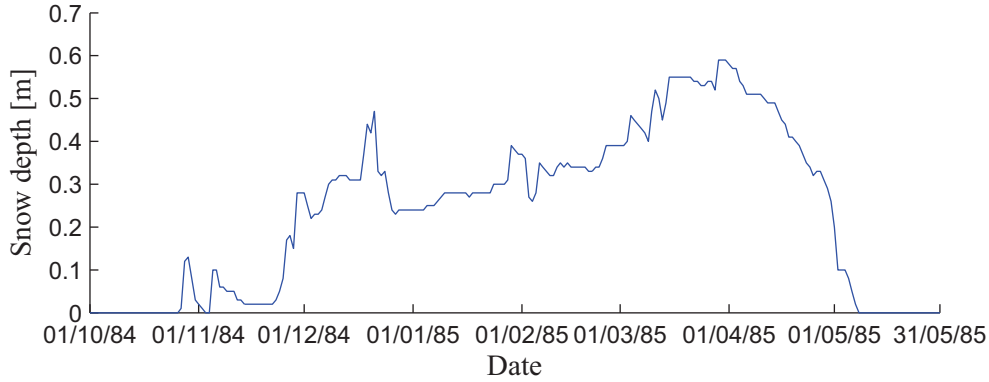

Figure 3.3: Snow depth at Luleå Airport in the winter 84/85 (SMHI 1985)

Where snow is present more factors has to be included in Stefan's law. The relation between ice growth and FDD then becomes:

$$FDD = \int_0^{h_i} l_f \rho_i \left(\frac{k_i h_s + k_s h_i}{k_i k_s} \right) dh_i \tag{3.2}$$

where k_s is the mean thermal conductivity of snow and h_s is the snow depth at time t.

An empirical formula, proposed by Zubov (1943) gives the following relation between ice growth and degree-days of freezing:

$$h_i^2 + 50h_i = 8FDD \tag{3.3}$$

The formula is based on observations from Russian polar stations, and is more sensitive to existing ice thickness than the analytic solution in Eq. (3.1). This makes the difference in calculated ice thickness between an exceptionally cold winter and an ordinary winter smaller than if e.g. Stefan's Law had been applied.

3.2 Numerical Model

3.2.1 Model Geometry

Björnklacken was 20.9 m high, and consisted if three main bodies. The lowest part of the lighthouse was a gravity base with a diameter of 12 m, and was filled with iron ore. The lower part of the central tower had a diameter of 2.9 m, and was approximately 10.6 m high. The slender upper part of the central tower had a diameter of 1.9 m, and was approximately 9.6 m high. A detailed dimensional sketch is shown in Figure 3.4.

The lighthouse was represented by a numerical model consisting of solid and shell elements, made in the FE-software ABAQUS. The solid sections, section 1 and 5 as shown in Figure 3.5, was modelled with C3D8R (Hibbit et. al.) reduced integration brick elements. All other sections consists of S4R (Hibbit et. al.) four-node shell elements. Detailed section division and accompanying element types are shown in Figure 3.5 and in Table 3.1.

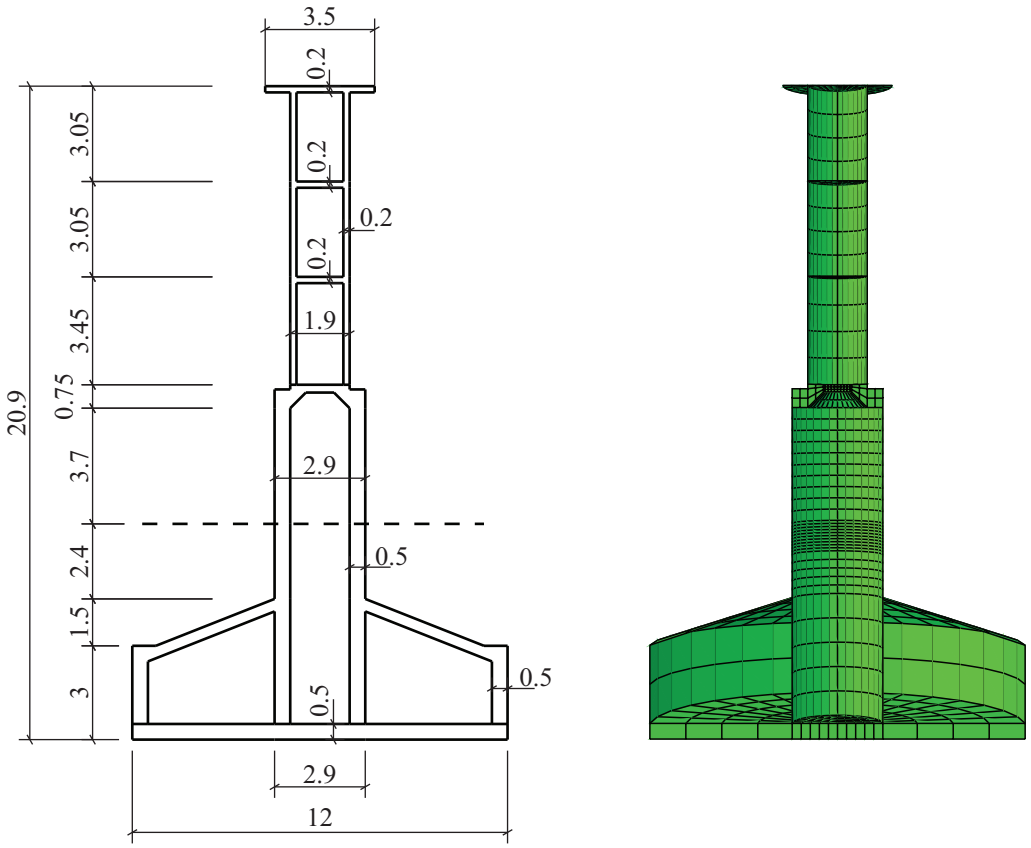

Figure 3.4: Dimensional sketch of Björnklacken lighthouse

To take into account the weight of the iron ore, the densitiy of the shell sections which forms the inner part of the tower has been increased. In addition, the weight of the outer part of the concrete slab forming the lower base, shown in Figure 3.5, has been adjusted in the same way. This is a modified version of the method proposed by Albrektsen (2008). The method has been adjusted to take into account the effect the location of the centre of gravity has on the structural analysis. The equivalent material densities are shown in Table 3.1. A concrete with density 2400 kg/m^3 was used as a basis when calculating equivalent densities. Buoyancy from the water displaced by the structure was applied using body loads on the sections of the structure which were submerged.

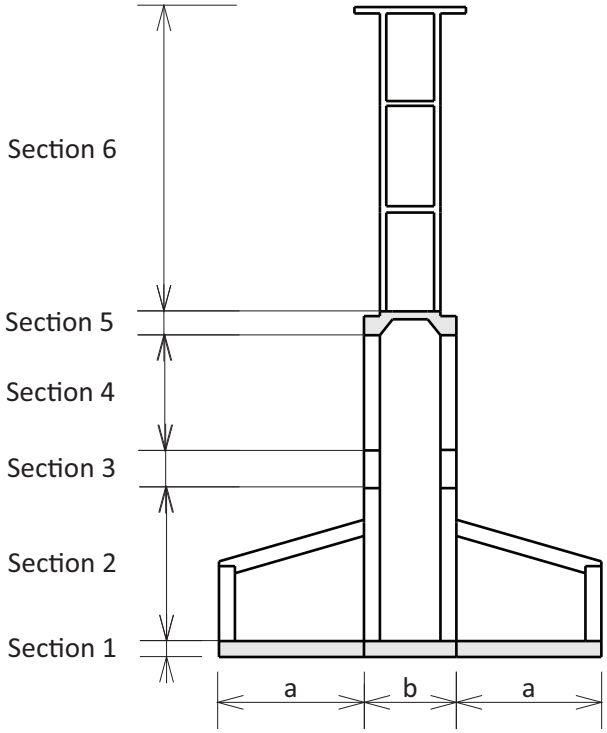

Figure 3.5: Lighthouse section division

A “top surface” discretization has been used when modelling the circular sections. Because of the procedure used by ABAQUS when calculating the mass of the structure, equivalent densities had to be introduced in all sections of the structure.

The stiffness of the shell elements in the loading area, shown as Section 3 in Figure 3.5 has been increased in the static analysis. The increase has been introduced to account for the contribution the iron-ore filling would have to resisting local deformations in the area the load is applied, and is given in Table 3.1.

Table 3.1: Material properties

Section	Element Type	Equivalent Density [kg/m^3]	Stiffness [Pa]
1a	C3D8R	15364	$3.4 \cdot 10^{10}$
1b	C3D8R	2400	$3.4 \cdot 10^{10}$
2a	S4R	2400	$3.4 \cdot 10^{10}$
2b	S4R	5172	$3.4 \cdot 10^{10}$
3	S4R	5172	$3.4 \cdot 10^{10}$
4	S4R	2193	$3.4 \cdot 10^{10}$
5	C3D8R	2400	$3.4 \cdot 10^{10}$
6	S4R	2274	$3.4 \cdot 10^{10}$

3.2.2 Element types

The numerical model of the lighthouse consists of two element types. These are described in the ABAQUS User's Manual (Hibbit et. al. 2008), and are:

- Reduced integration, 8-node cubic elements, C3D8R
- Reduced integration, 4-node shell elements, S4R

Figure 3.6 shows sketches of the element types. The solid parts of Björnklacken are made up of a total of 832 C3D8R elements, while the shell sections consists of 1920 S4R elements. A total of 3198 elements has been used.

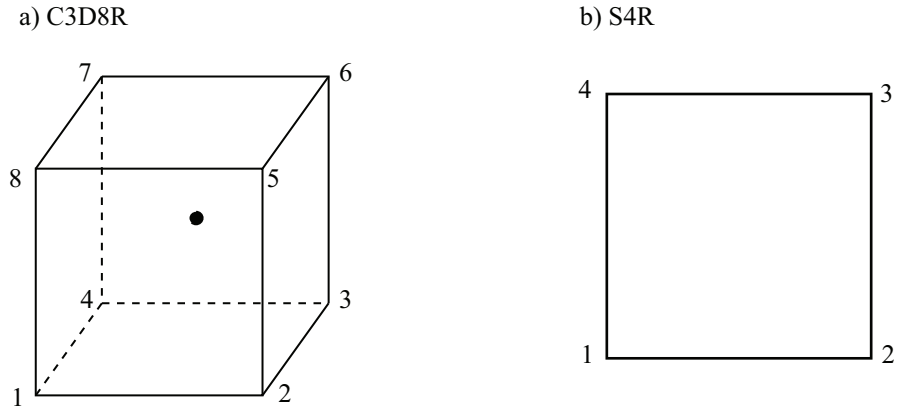

Figure 3.6: Element types

3.2.3 Seabed Modelling

Interaction

To simulate the soil-structure interaction, three models has been analyzed. Figure 3.7 shows sketches of the different interaction models. These are:

- A model where the base of the lighthouse has been fixed
- A model where the base of the lighthouse has been connected to a flexible seabed, using "TIE connectors" in ABAQUS/CAE,
- A model where the base of the lighthouse stands on top of a flexible seabed, only limited by the friction acting between the to entities

a) Base of lighthouse fixed, BF

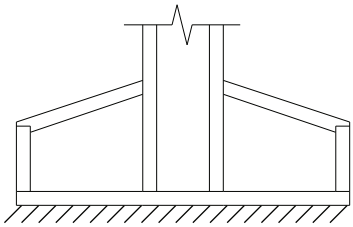

b) Flexible seabed, base of lighthouse constrained to seabed, FSC

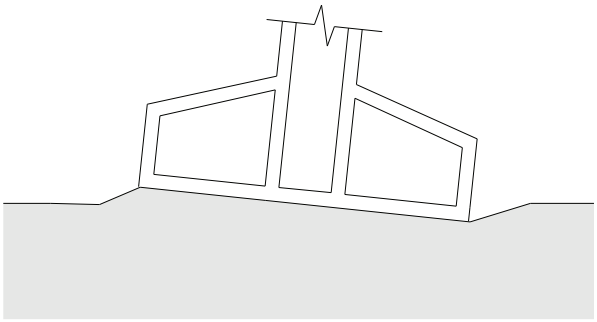

c) Flexible seabed, base of lighthouse unconstrained, FSU

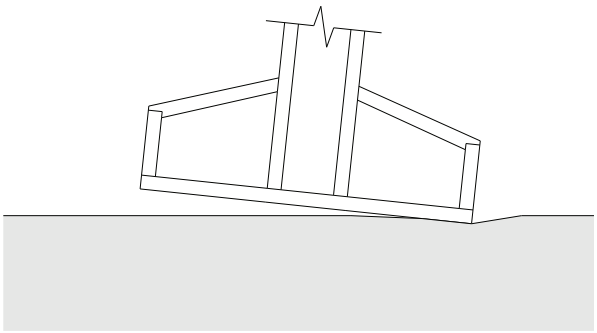

Figure 3.7: Ligthouse-seabed interaction types

In 3.7 b) and c), the seabed has been modelled as a flexible solid part, with properties found in accordance with recommendations from the geotechnical experts (Nordahl 2010). The seabed has a surface area of $3 \cdot D$ x $3 \cdot D$, were D is the diameter of the base of the lighthouse. Material

stiffness increases linearly over a depth equal to $2 \cdot D$. This has been discretizised by splitting the seabed into five layers of different stiffnesses, as illustrated in Figure 3.8.

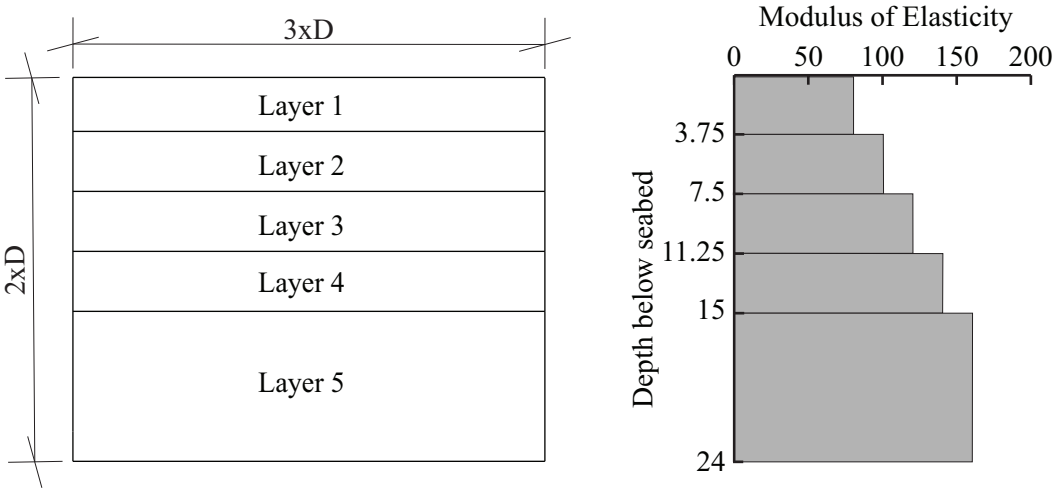

Figure 3.8: Stiffness of seabed

The section was meshed using reduced integration brick elements of the type C3D8R, and is shown in Figure 3.9.

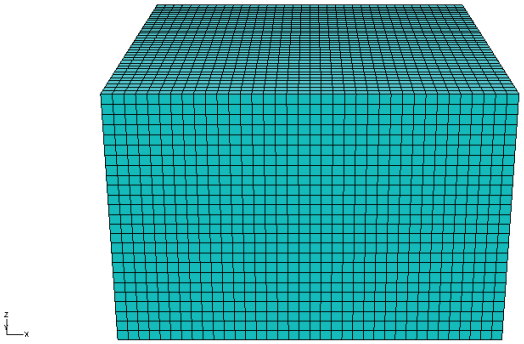

Figure 3.9: Discretizised seabed

Coefficient of Friction

The amount of force required to move the lighthouse in the horizontal direction is dependent on the magnitude of the frictional force acting between the lighthouse and the seabed. Frictional

force is dependent on the coefficient of friction. Coefficient of friction is dependent on the material of the seabed and the lighthouse, and the weight of the lighthouse. The relation between frictional force, friction coefficient and the weight of the structure can be expressed as:

$$F_f \leq \mu \cdot G \tag{3.4}$$

where μ is the coefficient of friction, F_f is the frictional force and G is the weight of the structure. According to recommendations from geotechnical experts a normal value for interaction between boulder clay and submerged concrete lies in the area 0.4-0.5 (Russell 2010). Figure 3.10 shows the relationship between μ and the corresponding frictional force.

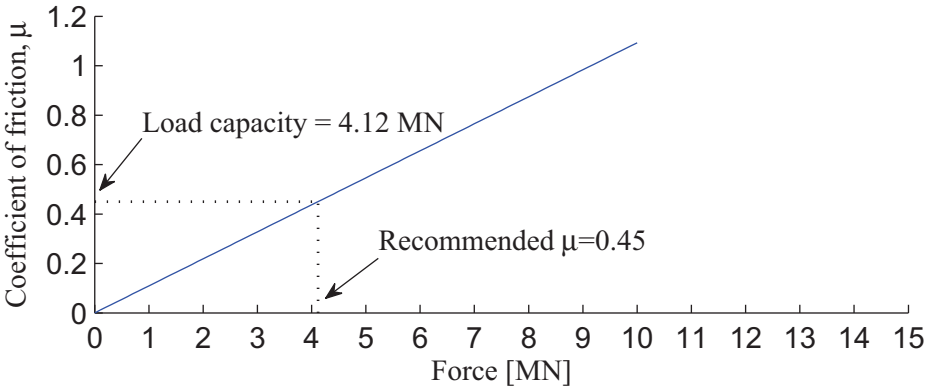

Figure 3.10: Load capacity if $\mu = 0.45$

3.3 Static Ice Loads

Static ice loads are in most cases regarded as an ice pressure, p_G, working over an area, A. The area is given as:

$$A = D \cdot h_i \tag{3.5}$$

Where D is the diameter of the structure, and h_i is the ice thickness. Ice pressure working on a structure with diameter D is illustrated in Figure 3.11.

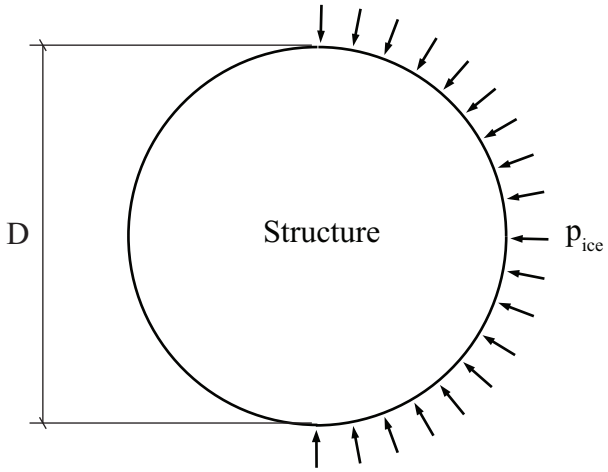

Figure 3.11: Static ice pressure (Albrektsen 2008)

The resulting force, F_G, can be regarded as a point load, and is calculated by multiplying the ice pressure with the area from Eq. (3.5). The formula for F_G is given as:

$$F_G = p_G \cdot D \cdot h_i \tag{3.6}$$

Approximately 90 percent of the ice lies below the surface. F_G has a point of attack in the middle of the ice, as shown in Figure 3.12. This means that for an ice thickness of one meter, the resultant force works on a point approximately 0.45 m below water level.

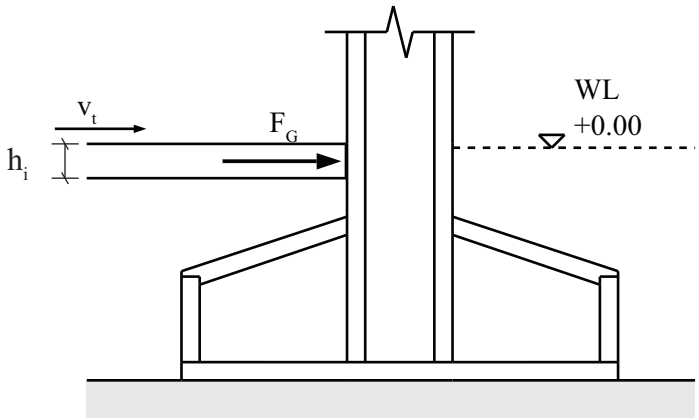

Figure 3.12: Static ice load working below sea level

3.4 Reinforcement in Critical Section

The critical section of Björnklacken has been defined as the cross-section in the transition between the central tower and the conic shaped gravity-base. The location of the critical section and the forces working in the critical section is shown in Figure 3.13.

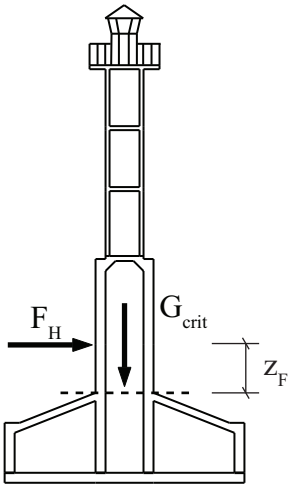

Figure 3.13: The lighthouse's critical section

The design moment working in the critical section, M_D, is dependent on the design. Different reports gives different design loads for Björnklacken, but for the purpose of calculating the reinforcement a report by Björk (1981) has been used as a source. Björk states a load which

Björnklacken was designed to handle before the rock-ancors were installed. The load is given as :

$$F_H = 2.5 \text{ MN/m} \tag{3.7}$$

M_D is then defined as:

$$M_D = F_H \cdot z_F \tag{3.8}$$

where z_F is the lever arm between the loading point and the critical section. In addition to the moment, a gravity load, G_{crit}, works on the section. G_{crit} is given as the weight of the parts of the structure which lies above the critical section.

3.5 Modal Analysis

A modal analysis is carried out to determine the characteristics of the eigenmodes most probable to occur under dynamic ice-loads. Typically, the lowest structural eigenmodes are the modes most susceptible to self-excited vibrations (Kärnä 2006).

The modal analysis was performed on the models where FB and FSC discretization had been used. The model where the lighthouse was unconstrained could not be the subject of a modal analysis because of rigid body moves.

To find the eigenmodes of interest, a frequency analysis has been carried out in ABAQUS. Both the fixed-base model and the model where the base of the lighhouse is constrained to the seabed has been analysed. The frequency analysis was also used to determine frequencies, generalised masses, and modal amplitudes for the ten lowest structural eigenmodes. Eigenmodes involving mainly the distortion of seabed elements has been ignored when selecting eigenmodes and data for further use.

3.6 Dynamic Ice Loads

3.6.1 SDOF-system

The eigenmodes found through modal analysis can be studied separately by simplifying the problem as a single degree of freedom (SDOF) problem. Higher and lower modes may influence

the behaviour of a structure, but SDOF-system is often sufficient to analyse dynamic response (Sodhi 1988).

To study the dynamic problem as a SDOF-system, the dynamic loading equation has to be simplified. Kärnä (2006) considered the problem shown in Figure 3.14, where he decomposed the ice force into two components given as:

$$F_c(t) = F_{CM} + F_{CD}(t) \tag{3.9}$$

where F_{CM} is the static mean ice force and $F_{CD}(t)$ is the time varying ice force.

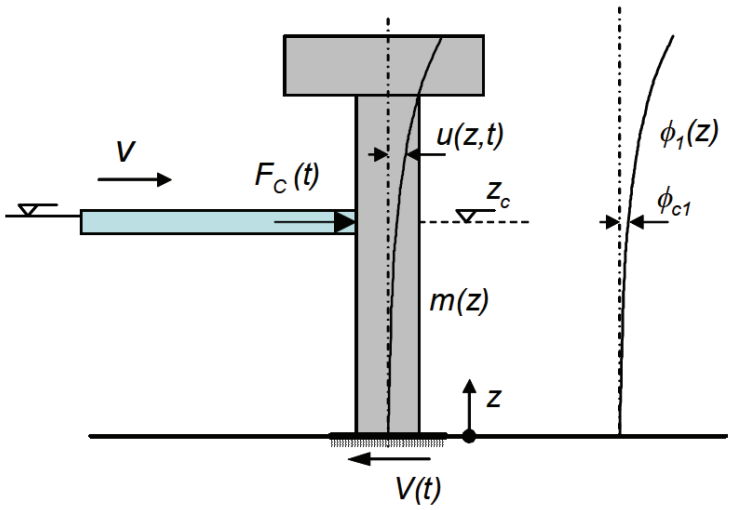

Figure 3.14: SDOF-system 2 (Kärnä et. al. 2006)

The equation of equilibrium for the dynamic equation is written as:

$$\mathbf{M}\ddot{\mathbf{u}}(t) + \mathbf{C}\dot{\mathbf{u}}(t) + \mathbf{K}\mathbf{u}(t) = \mathbf{F_c}(t) \tag{3.10}$$

where $\mathbf{M}$ is the mass matrix, $\mathbf{C}$ is the damping matrix and $\mathbf{K}$ is the stiffness matrix. $\mathbf{u}(t)$ is the displacement vector and $\mathbf{F_c}(t)$is the external forces vector. $\ddot{\mathbf{u}}(t)$ and $\dot{\mathbf{u}}(t)$ are the acceleration and speed vectors.

Using results from an eigenvalue analysis, the equation of motion is transformed to a generalised coordinate system using the relation:

$$\mathbf{U}(t) = \Phi\mathbf{R}(t) \tag{3.11}$$

where $\Phi = [\varphi_1 \varphi_2 .... \varphi_n]$ is a matrix where n eigenmodes are included and $\mathbf{R}$ is a vector containing generalised displacements. After transformation, Eq. (3.10) is written as:

$$\mathbf{M}^*\ddot{\mathbf{R}}(t) + \mathbf{C}^*\dot{\mathbf{R}}(t) + \mathbf{K}^*\mathbf{R}(t) = \mathbf{Q}(t) \tag{3.12}$$

where

$$\mathbf{M}^* = diag(M_n^*)$$

$$M_n^* = \phi_n^T M \phi_n \cong \int m(z)\phi_n^2(z)dz$$

$$\mathbf{C}^* = diag(2\xi_n \omega_n M_n)$$

$$\mathbf{K}^* = diag(\omega_n^2 M_n) \text{ and}$$

$$\mathbf{Q} = \Phi^T F_D$$

and $\dot{\mathbf{R}}(t)$ and $\ddot{\mathbf{R}}(t)$ are vectors containing time dependent generalised velocities and accelerations. The damping coefficient, ξ_n is defined as the ratio of damping in eigenmode n compared to critical damping. The angular frequency of eigenmode n, ω_n is equal to $\omega_n = 2\pi \cdot f_n$.

Considering only the first mode of vibration, Eq. (3.12) can be written as:

$$M_1^*\ddot{R}_1(t) + 2\xi_1\omega_1 M_1^*\dot{R}_1(t) + \omega_1^2 M_1^* R_1(t) = Q_1(t) \tag{3.13}$$

The eigenmode is then scaled to unity at water level and the notation for $R_1(t)$ is then changed using the by using the expressions:

$$\psi(z) = \frac{\phi_1(z)}{\phi_{1c}}\,,\ \phi_{1c} = \phi_1(z_c) \tag{3.14}$$

and

$$u_c(t) = \phi_{1c} R_1(t) \tag{3.15}$$

where $u_c(t)$ is the displacement at the area where the ice is on contact with the structure. The expressions in Eq. (3.14) and (3.15) is then implemented in Eq. (3.13). The equation of motion can now be written as:

$$\phi_{1c}^2 \int m(z)\psi^2(z)dz \left\{ \frac{1}{\phi_{1c}} \left[u_c(t) + 2\xi_1\omega_1 u_c(t) + \omega_1^2, u_c(t) \right] \right\} = \phi_{1c} F_{CD}(t) \tag{3.16}$$

This equation can be written as the equation of motion for a single-degree-of-freedom system:

$$M_n\ddot{u}(t) + C_n\dot{u}(t) + K_n u(t) = F_{CD}(t) \tag{3.17}$$

where the modal mass, M, is dependent on the generalized mass, M_n^* and the modal amplitude, ϕ_n, of the eigenmode. The equation for modal mass is written as:

$$M_n = \frac{M_n^*}{\phi_n^2} \tag{3.18}$$

The damping factor, C_n, is introduced as a function dependent on ξ_n, ω_n, and M_n. The expression for damping can be written as:

$$C_n = 2\xi_n\omega_n M_n \tag{3.19}$$

Modal stiffness is dependent on M_n and ω_n, and is defined as:

$$K_n = \omega_n^2 M_n \tag{3.20}$$

Eq. (3.17) can now be used to describe the motion of the generalised system shown in Figure 3.15. The SDOF-model is used as a basis for all dynamic analyses performed in this project.

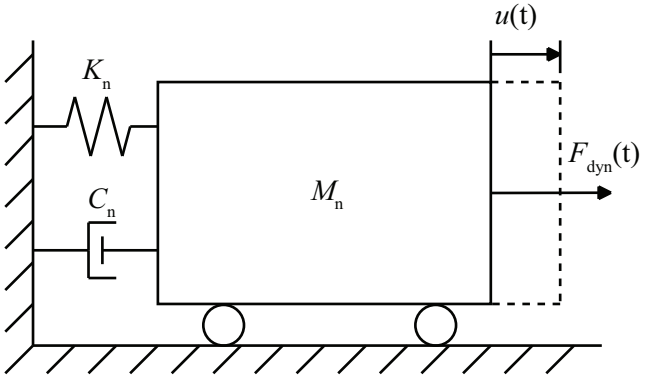

Figure 3.15: SDOF-model

Using Newmark's method (Chopra 2007), the displacement, velocity and acceleration of the SDOF-system at time t can be found by Eq. (3.21) and (3.22).

$$\dot{u}_{i+1} = \dot{u}_i + [(1-\gamma)\Delta t]\ddot{u}_i + (\gamma\Delta t)\ddot{u}_{i+1} \tag{3.21}$$

$$u_{i+1} = u_i + (\Delta t)\dot{u}_i + [(0.5-\beta)(\Delta t)^2]\ddot{u}_i + [\beta(\Delta t)^2]\ddot{u}_{i+1} \tag{3.22}$$

If the factors β and γ are taken as 1/4 and 1/2, the equations yields the constant acceleration method, an uncoditionally stable solution method. The constant acceleration method has been used in the current work. Examples of forcing functions used to simulate dynamic response is given in Figure 3.16 and 3.17.

3.6.2 Damping

A lower bound limit of $\xi = 0.02$ and an upper bound limit of $\xi = 0.01$ for the damping fraction is suggested for dynamic analysis in a report by Kärnä (2006). In the dynamic analyses of the present work, a damping fraction of $\xi = 0.02$ has been used for illustrating dynamic response. Dynamic amplification factors have been found using both higher and lower damping fractions.

3.6.3 Dynamic Amplification Factor

The dynamic amplification factor, DAF, describes the ratio between the dynamic and static response. The same F_G is used in both the static and dynamic analysis. DAF for a numerical model can be expressed simply as:

$$DAF = \frac{u_{dyn,max}}{u_{static}} \tag{3.23}$$

where $u_{dyn,max}$ is the steady-state solution for the dynamic amplitude, and u_{static} is the static response.

3.7 Design Codes

3.7.1 International Organization for Standardization - ISO

The recently issued ISO/DIS 19906 design code (ISO 2009), provides recommendations and guidance for both the construction, design and other parts of the building process related to offshore structural design. The ISO-code includes standardized design loads for both static and dynamic ice loading.

Static

Static ice load in the ISO-code is given by an ice pressure

$$p_{G,ISO} = C_R h^n \left(\frac{D}{h}\right)^m \tag{3.24}$$

where C_R is the ice strength coefficient, D the width of the structure, h the ice thickness, and m and n are empirical exponents. A recommended value for C_R is 1.8 for stiff structures in the Baltic Sea (ISO 2009). This value has been when calculating static loads in the current work. Suggested values for m and n are given in the ISO-code as:

$$m = 0.16$$

$$n = -0.5 + h/5 \text{ for h} < 1.0 \text{ m}$$

$$n = -0.3 \text{ for h} \geq 1.0 \text{ m}$$

Dynamic

If static analysis predicts a displacement of 10 mm or more, the structure needs to be checked for dynamic effects. The ISO-code states that the natural modes most susceptible to ice-induced vibrations, typically the lowest ones, should be checked for dynamic instability. A stability criterion is also given in to help evaluate susceptible modes. The stability criterion is dependent on the characteristics of each fundamental mode and the damping ratio, ξ. The damping ratio for a natural mode should generally be higher than the the stability criterion to avoid dynamic instability. The criterion is given as:

$$\xi_n \geq \frac{\phi_{nC}^2}{4\pi f_n M_n} \cdot h \cdot \theta \tag{3.25}$$

Where ξ_n is the damping ratio, ϕ_{nC}^2 the modal amplitude at the level of the loading point, f_n the natural frequency and M_n the modal mass of an eigenmode, while θ is a stability coefficient. The ISO-code suggests that the stability coefficient is set to $\theta = 40 \cdot 10^6$ kg/(m·s), based on field data from narrow structures in the Baltic Sea.

If frequency lock-in occurs, a forcing function, shown in Figure 3.16, is used to apply the load and determine the dynamic response of the structure.

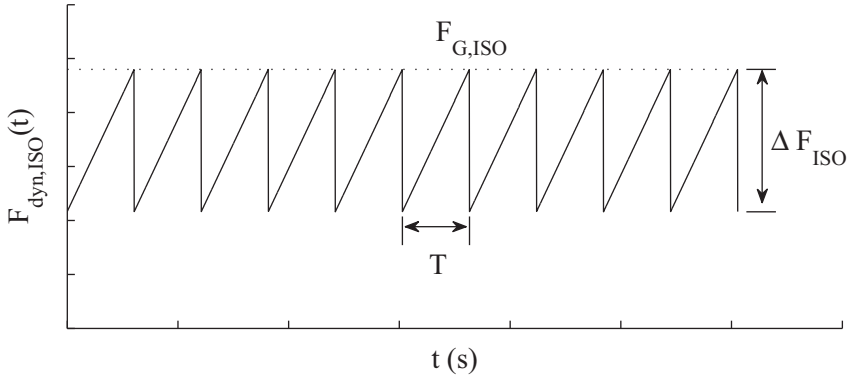

Figure 3.16: Simplified forcing function (ISO 2009)

The amplitude of the forcing function in Figure 3.16 is given by ΔF_{ISO}, which can be calculated using the formula:

$$\Delta F_{ISO} = qF_{max,ISO} \tag{3.26}$$

where the peak force $F_{max,ISO} = F_{G,ISO}$. The amplitude fraction, q, should initially be taken as a value between 0.1 and 0.5 and later be scaled based on the response analysis. According to the ISO-code the factor should be scaled so that the velocity response at the waterline amounts to a value that is 1.4 times the highest ice velocity,v_t , at which a lock-in condition can occur. The ice velocity can be calculated by the equation:

$$v_t = \gamma_v f_n \tag{3.27}$$

Where $\gamma_v = 0.0600$ m, and f_n is the natural frequency of the eigenmode.

The dynamic force function is then given by the sawtooth function:

$$F_{dyn,ISO} = F_{G,ISO} + \Delta F_{ISO} \cdot (\text{sawtooth}(2\pi \cdot f_n t) - 1) \tag{3.28}$$

3.7.2 The International Electrotechnical Commision - IEC

The design code “Wind Turbines - Part 3: Design requirements for offshore wind turbines” (IEC 2009) specifies design requirements for offshore wind turbines. For the purpose of designing structures in an arctic enviroment, general formulas for both static and dynamic ice loads are given.

Static

The static part of the ice load according to the IEC-code is dependent on a number of constants, ice thickness, diameter of the structure and the crushing strength of the ice in a given area. It is given by the formula:

$$F_{G,IEC} = k_1 k_2 k_3 k_4 h_i D \sigma \tag{3.29}$$

where k_1 is the shape factor, taken as 0.9 for a circular shaped structure. k_2 is the ice contact factor, taken as 0.5 when the ice is continuously moving. k_3 is the factor for the ratio between the ice thickness and the structure diameter, taken as $\sqrt{1+5h_i/D}$. σ_c is the crushing strength of the ice, determined from statistical data if available. If no statistical data is available the ice crushing strength can be taken as 3.0 MPa for ice in motion at the coldest time of the year.

Dynamic

Dynamic loading is represented by a sinusoidal harmonic forcing function, given in Equation 3.30.

$$F_{dyn,IEC} = F_{G,IEC}\left(\frac{3}{4} + \frac{1}{4}\sin\left(2\pi f_n t\right)\right) \tag{3.30}$$

The equation shows that the dynamic forcing function is dependant on the static load contribution, $F_{G,IEC}$, given in Equation 3.29, and the frequency of the ice loading, f_n. A forcing function with frequency f and static load $F_{G,IEC}$ is shown in Figure 3.17.

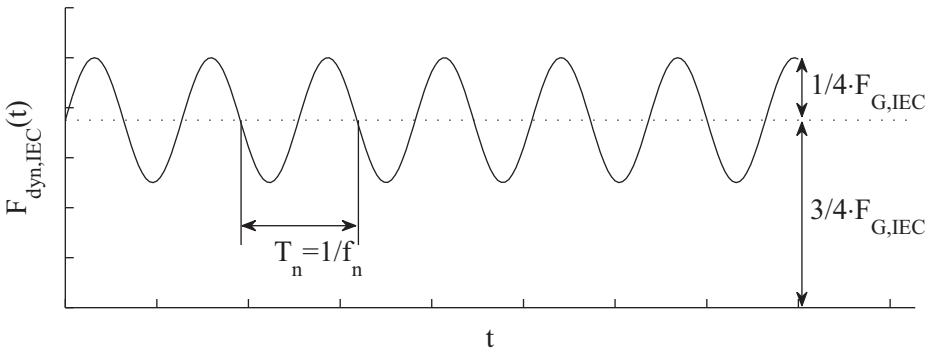

Figure 3.17: Dynamic effect from ice loading (IEC 2009)

3.7.3 American Petroleum Institute - API

The design code "Recommended Practice for Planning, Designing, and Constructing Structures and Pipelines for Arctic Conditions" (API 1995), contains recommendations and guidelines for the whole planning and designing process of offshore structures in an arctic enviroment. The API-code's recommendations for calculating static ice loads has been used in the current work.

Static

The static ice load is, in the same fashion as in the ISO-code, calculated as an ice pressure, p_G, given by the formula:

$$p_{G,API} = \frac{8.1}{\sqrt{Dh_i}} \tag{3.31}$$

In contrast to the ISO- and the IEC-code, static ice pressure found using the API-code increases with lower structural diameter.

3.7.4 Other Work

Bjerkås (2007)

In an article by Bjerkås (2007), it is proposed an upper bound static ice pressure for use as an indicative tool for estimating ice pressure on structures with known width. The equation is given in Eq. (3.32), and is dependent on structural width, D, only.

$$p_{G,\text{Bjerkås}} = 2.05D^{-0.06} \tag{3.32}$$

Engelbrektson (1987)

In the report by Engelbrektsson and Fransson (1987), the formula for the design ice load for lighthouses built in the same period as Björnklacken, was defined as:

$$F_D = 4 + 2.3 \cdot D \tag{3.33}$$

which is a simplification of:

$$F_D = 1.6 \cdot \sqrt{1 + 5 \cdot \frac{h}{D}} \cdot h \cdot D \tag{3.34}$$

where h is the ice thickness, and D is the diameter of the structure.

Kärnä (2006)

In the report "How to use saw-tooth force functions to model self-excited vibration" (Kärnä 2006), a method to enhance the accuracy of the sawtooth model is suggested. A new formula for ΔF is given as:

$$\Delta F_{\text{Kärnä}} = \frac{2\beta}{\gamma(\alpha) \cdot \pi} \cdot \frac{\xi_n K_n}{f_n} v_t \tag{3.35}$$

where β is a factor correlating ice velocity and the velocity amplitude at waterline, set to $\beta = 1$ for further analysis, in accordance with Engelbrektsons findings. $\gamma(\alpha)$ is a correction factor dependent on a shape factor, α. The shape factor for the sawtooth function given in the ISO-code is $\alpha = 1$. Kärnä's report does not supply a correction factor for shape factors higher than $\alpha = 0.95$, but has been found as $\gamma(1) = 0.6391$ through extrapolation of known values.

4 Results

4.1 Ice Thickness

The formulas to determine the ice thickness are given in Eq. (3.1), (3.2) and (3.3). Recordings of the temperature at the exact location of Björnklacken are unavailable. Therefore temperature data at Luleå Airport, given in Figure 3.1, has been used to estimate the ice thickness. Estimations of the ice growth according to the different equations are given in Figure 4.1.

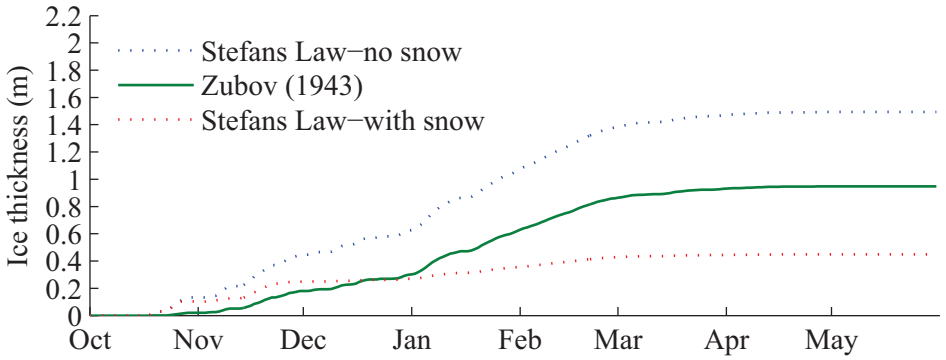

Figure 4.1: Ice growth around Björnklacken in the winter 1984/-85

According to previous data, the empirical equation proposed by Zubov, shown as a solid line in Figure 4.1, is reliable for computing ice thickness at sea and was therefore used as a guideline when the ice thickness was assumed. For the 4th of April 1984 Zubov's equation yields an ice thickness of roughly 0.93m.

Ice thickness each year, estimated using the formula proposed by Zubov (1943), is presented in Figure 4.2. The ice thickness varies from a minimum value of 0.50 m in 1992 to a maximum of 1.22 m in 1966. In Björnklacken's first winter of operation, 1969/70, the ice thickness reached a maximum of approximately 0.91 m. The mean ice thickness for the whole period (1965-1995) is 0.79 m, with a standard deviance of approximately 0.15 m.

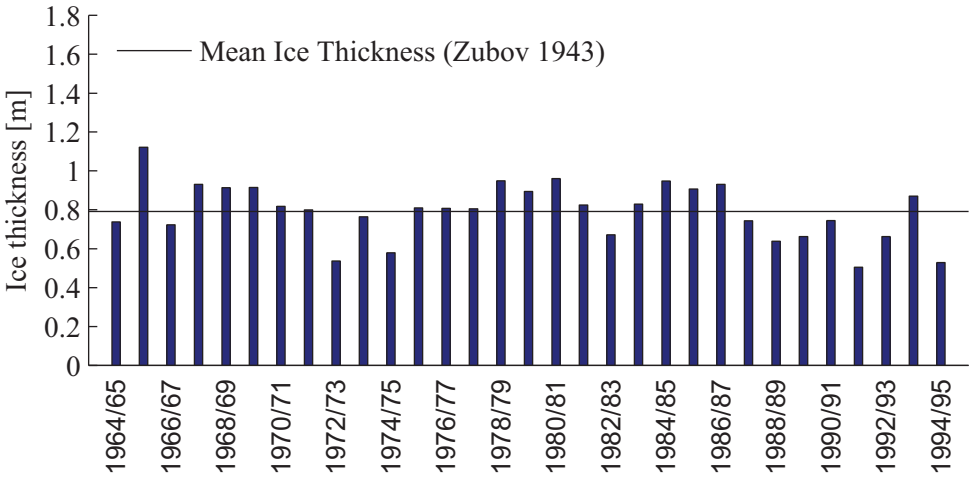

Figure 4.2: Ice thickness per year, as proposed by Zubov (1943), for the period 1965-1995

4.2 Static Analysis

4.2.1 Choice of seabed discretization

The choice of discretization used when modelling the lighthouse-seabed interaction plays a major part in evaluating the structural response of the lighthouse due to static ice loading. Figure 4.3 shows displacement at waterline for the different lighthouse-seabed interaction types. Using both interaction type a) and b) leads to a linear relation between load and displacement. The relation is not linear if interaction type c) is used since the lighthouse starts to overturn when the load magnitude exceeds approximately 2 MN.

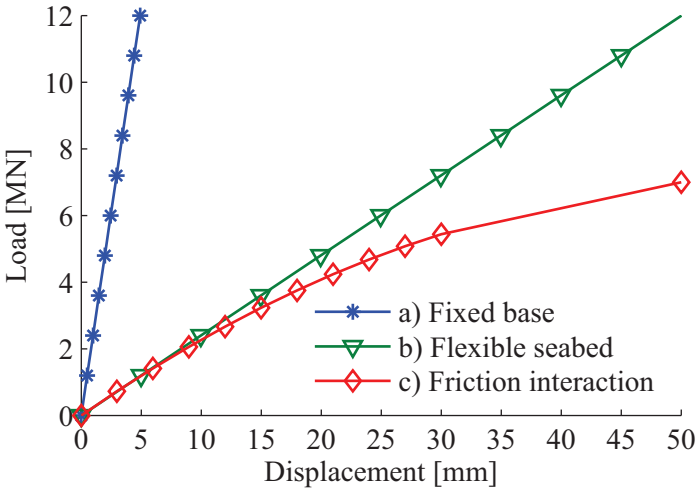

Figure 4.3: Load vs. Displacement for the different models

4.2.2 Design Codes

The static ice loads calculated according to the different design codes covered in Section 3.7, can all be related to the ice-thickness. In Figure 4.4 a), the relation between ice thickness and static ice loads calculated using the different design codes is shown.

When an ice thickness of one meter is assumed, static ice loads calculated in accordance with the IEC-code and the method proposed by Bjerkaas (2006) are very similar, predicting loads of 6.46 and 6.34 MN. The load calculated using the ISO-code is 4.40 MN, while the API-code predicts a static ice load of 14.48 MN.

A plot presenting the relation between ice-thickness and displacement of the lighthouse at water level is shown in Figure 4.4 b). The displacement at waterline has been found using a model

where the seabed is discretizised as a solid part and where the base of the lighthouse has been constrained to the seabed.

If the static ice load causes a displacement of more than 10 mm, the ISO-code states that dynamic amplification has to be taken into account. In Figure 4.4 b), the 10 mm limit is shown as a dotted line. If the static ice load is calculated according to the ISO-code, dynamic effects have to be analysed when the ice thickness exceeds 0.45 m. If the same criterion for dynamic effects is used for the IEC-code, dynamic analysis has to be performed when the ice thickness exceeds 0.50 m.

a) Ice thickness vs. load magnitude

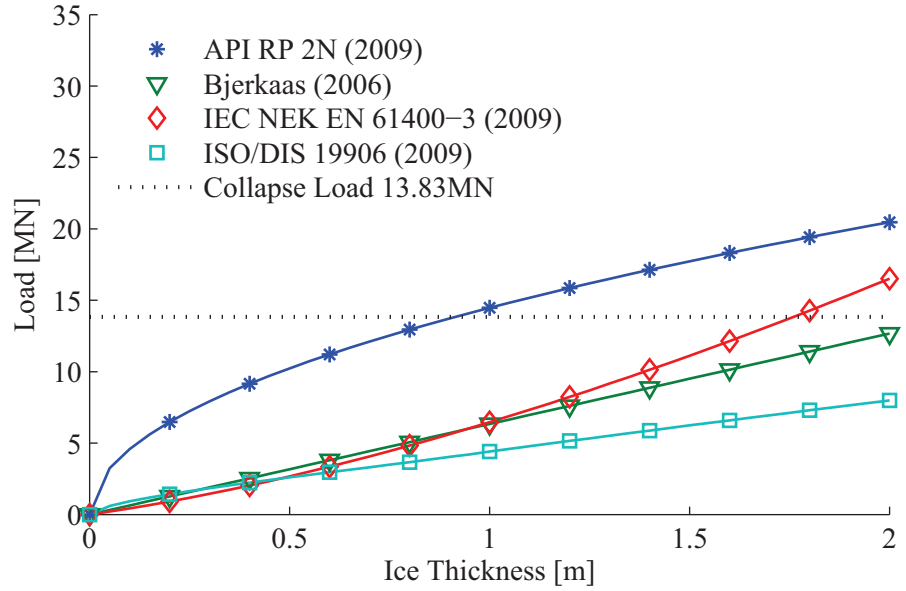

b) Ice thickness vs. displacement at waterline

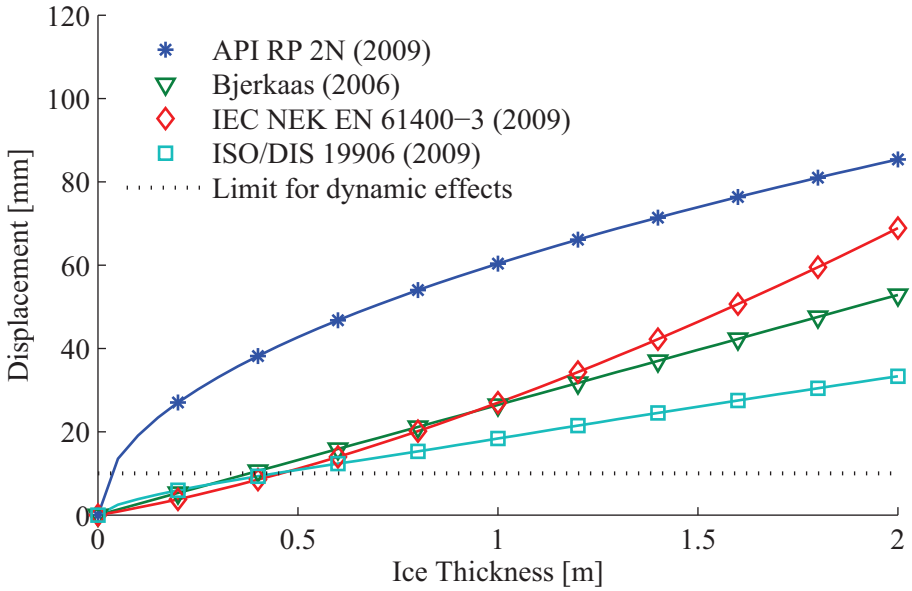

Figure 4.4: Ice thickness plotted against displacement and load magnitude

4.2.3 Collapse moment

The collapse moment of Björnklacken was the moment which caused the rock ancors to break. The forces contributing to Björnklacken's resistance to overturning were:

- Prestressed rock anchors, four tendons, each with seven strands and an ultimate strength of 200 kN
- The weight of the concrete
- The weight of the iron ore filling

These forces can be simplified as a single resultant force acting in the centre of the structure, with a lever arm shown as x_G in Figure 4.5. The static ice force, assumed to act approximately 0.50 m below waterline has a lever arm shown as z_P in the figure.

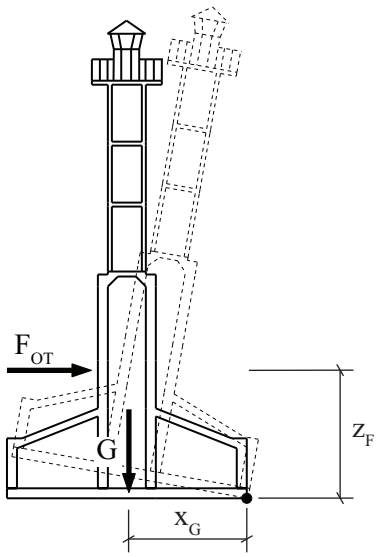

Figure 4.5: Collapse moment

The volume, density and the weight of the concrete and the iron ore, as well as the buoyancy caused by displaced water, is presented in Table 4.1. Density of the iron ore filling is based on the report from Engelbrektson (1987). It is worth noting that the weight of the structure calculated in this report is somewhat higher than the weight calculated by Engelbrektson. Engelbrektsson reported a total weight of 8.7 MN, approximately 5% lower than the total weight calculated in Table 4.1.

Table 4.1: Mass calculations

Material	Total Volume [m^3]	Density [kg/m^3]	Mass [kg]	Weight [MN]
Concrete	194.0	2400	465709	4568606
Iron Ore	231.9	3300	765142	7506046
Water	297.7	1000	297664	2920082
Total			933188	9154570

Using the calculated weight of the total structure, the ultimate strength of the prestressed tendons, and lever arms of $x_G = 6$ m and $z_P = 6.4$ m, this computes to the following overturning force:

$$F_{OT} = \frac{(4 \cdot 7 \cdot 0.20 \text{ MN} + 9.15 \text{ MN}) \cdot 6 \text{ m}}{6.4 \text{ m}} = 13.83 \text{ MN}$$

4.2.4 Reinforcement in Critical Section

Since Björnklacken's collapse came as a result of an overturning moment, thorough investigation of reinforcement and stresses has not been performed. An amount of reinforcement, and the stresses in the cross-section has been checked using a script developed by Lehmann (2010). The script calculates the stresses in accordance with NS3472 and was developed as a part of his Master's Thesis. The calculations has been performed without regards to the pre-stressed rock-anchors, which were added after movement along the seabed was detected during the spring of 1970 (Björk 1981).

Using the serviceability load given in Eq. (3.7) for Björnklacken, which has a diameter of 2.9 m, the load can be calculated as:

$$F_H = 2.5 \cdot 2.9 = 7.25 \text{ MN}$$

Based on the dimensional sketch given in Figure 3.4, the critical section lies approximately 2.4 m below waterlevel. Assuming an ice thickness of one meter, which has a loading point approximately 0.4 m below waterlevel, the design moment from Eq. (3.8) is given as:

$$M_D = 7.25 \cdot 2.0 = 14.5 \text{ MN}$$

The weight of the parts of the structure which lies above the critical section, shown as G in Figure 3.13, is calculated to be:

$$G_{crit} = 0.54 \text{ MN}$$

The reinforcement has been assumed to be of normal quality with a yield strength of $f_y = 500 \text{ N/mm}^2$. Two layers of 16 mm rebars with centre distance of 50 mm proved to be sufficient for the given horizontal design load. Approximate rebar placement is shown in Figure 4.6.

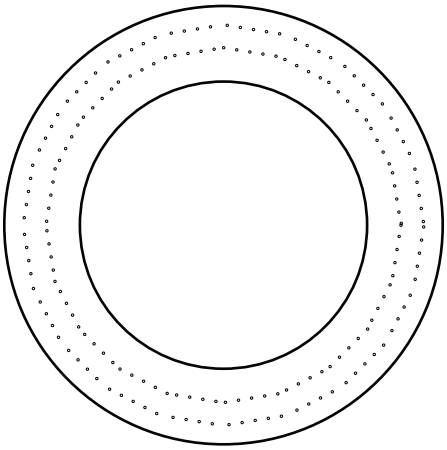

Figure 4.6: Distribution of reinforcement (Illustration only, not measureable)

4.2.5 Lateral displacement

The lateral displacement which occured after the rock anchors broke is dependent on the magnitude of friction between the lighthouse and the seabed. In Figure 4.7 ice thickness has been plotted against coefficient of friction, μ. Only the ISO code fails to predict lateral displacement if $\mu = 0.45$ and the ice thickness is 0.93 m. Dynamic amplification has not been taken into account in the figure.

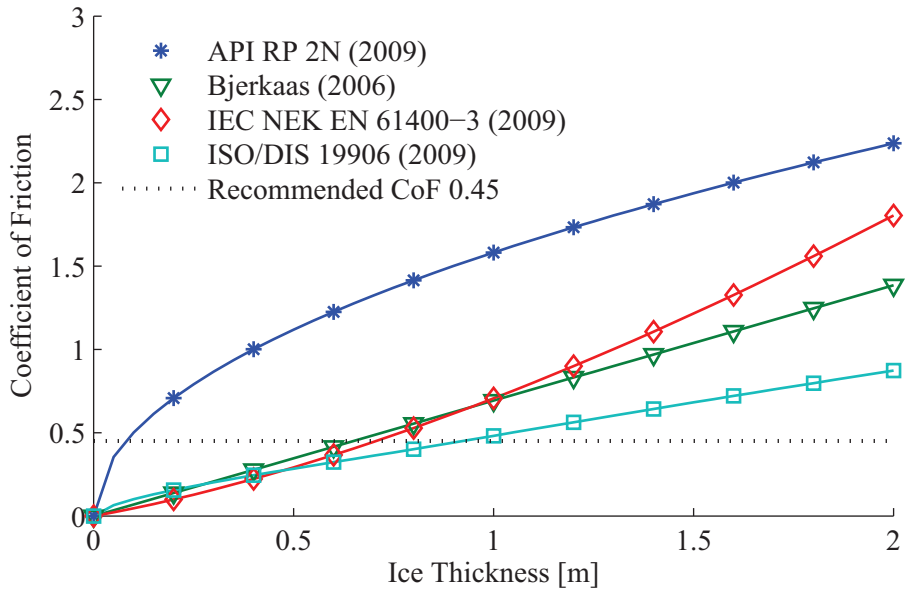

Figure 4.7: Coefficient of friction plotted against ice thickness

4.3 Modal Analysis

4.3.1 Fixed Base

Modal analysis of the lighthouse when FB-discretization has been used is primarily interesting to investigate which eigenmodes are typical for the structure. Since a seabed has not been included in the model, the eigenmodes are solely structural.

Modes 1 and 2 involve a slight tilting of the central tower. The modes are identical, with fundamental frequencies of $f_1 = f_2 = 5.2591$ Hz. Modal amplitudes for mode 1 and 2 are $\phi_1 = \phi_2 = 0.0347$.

a) Eigenmode 1, $f_1 = 5.2591$ Hz

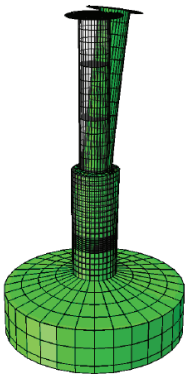

a) Eigenmode 2, $f_2 = 5.2591$ Hz

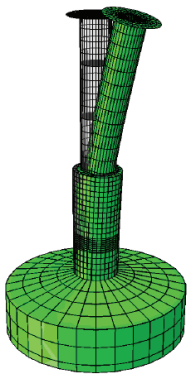

Figure 4.8: Fixed base, eigenmodes 1 and 2

Eigenmodes 3 and 4 gives large deformations, involving both rotation and deformations of the tower. They have identical fundamental frequencies, $f_3 = f_4 = 18.956$ Hz. Modal amplitudes vary slightly and are $\phi_3 = 0.4357$ and $\phi_4 = 0.4364$.

a) Eigenmode 3, $f_3 = 18.956$ Hz

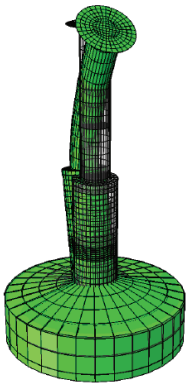

a) Eigenmode 4, $f_4 = 18.956$ Hz

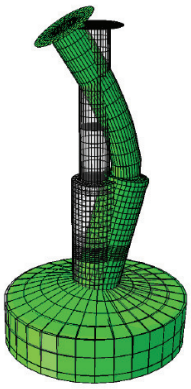

Figure 4.9: Eigenmodes 3 and 4

In mode 5 the centre tower is rotated while the lighthouse base stays undeformed, meaning very small deformations in lateral direction. The fundamental frequency of the mode is $f_5 = 35.290$ Hz, and the modal amplitude is $\phi_5 = 0.0496$. Mode 6 involves only the elongation of the centre tower. It has $f_6 = 41.981$ Hz and a modal amplitude of $\phi_6 = 0.0019$.

a) Eigenmode 5, $f_5 = 35.290$ Hz

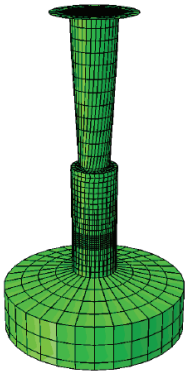

a) Eigenmode 6, $f_6 = 41.981$ Hz

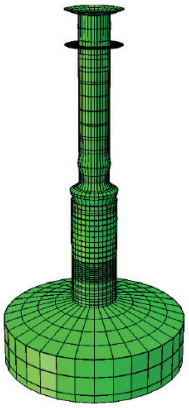

Figure 4.10: Eigenmodes 5 and 6

Eigenmode 7 and 8 are almost identical, with rotations and large deformations of the tower. Both

modes have $f_7 = f_8 = 44.158$ Hz. Modal amplitudes are $\phi_7 = 0.3602$ and $\phi_8 = 0.3598$.

a) Eigenmode 7, $f_7 = 44.158$ Hz

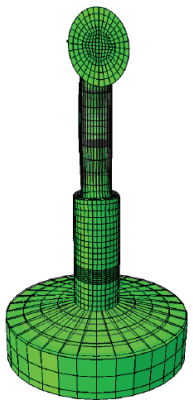

a) Eigenmode 8, $f_8 = 44.158$ Hz

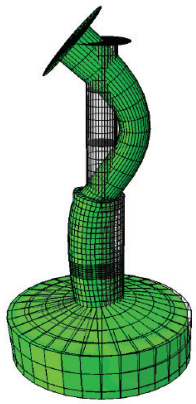

Figure 4.11: Eigenmodes 7 and 8

The eigenmodes 9 and 10 are similar to modes 7 and 8, but have a more evident sinusoidal shape. Deformations of the upper parts of the lighthouse base also occur. Fundamental frequencies are $f_9 = f_{10} = 58.035$ Hz for both modes and modal amplitudes are $\phi_9 = 0.2023$ and $\phi_{10} = 0.2046$.

a) Eigenmode 9, $f_9 = 58.035$ Hz

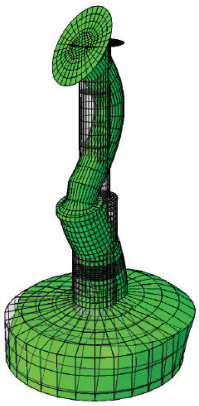

a) Eigenmode 10, $f_{10} = 58.035$ Hz

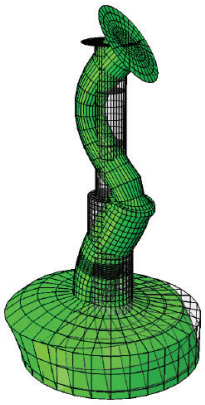

Figure 4.12: Eigenmodes 9 and 10

Table 4.2 shows a summary of the data from the modal analysis. The lowest fundamental frequencies of the ten first eigenmodes is $f_1 = 5.2591$. High frequencies combined with low modal amplitudes at load level makes the risk for frequency lock-in very low. These results have therefore not been used for further analyses.

Table 4.2: Frequency, generalized mass and modal amplitude, FB discretization

Eigenmode	Frequency [rad/sec]	Frequency [1/sec]	Modal amplitude, ϕ_n	Generalized mass
1	33.044	5.2591	0.0347	21928
2	33.044	5.2591	0.0347	21928
3	119.10	18.956	0.4357	72872
4	119.10	18.956	0.4364	72872
5	221.73	35.290	0.0496	6881
6	263.77	41.981	0.0019	26103
7	277.45	44.158	0.3602	37005
8	277.45	44.158	0.3598	37005
9	364.65	58.035	0.2023	48160
10	364.65	58.035	0.2046	48160

4.3.2 Flexible Seabed

A modal analysis of the model with flexible seabed and constrained base returns both structural eigenmodes and eigenmodes were the seabed is distorted. Only modes which are structure-specific are evaluated for dynamic effects. Therefore, the modes without noteworthy structural displacements are disregarded and not included in the current work.

Eigenmodes 1 and 2 are identical, but are displaced in different directions. The modes involve a tilting of the tower and a modal amplitude of $\phi_1 = \phi_2 = 0.2185$ at loading point. Both modes have a fundamental frequency of $f_1 = f_2 = 3.3023$ Hz.

a) Eigenmode 1, $f_1 = 3.3023$ Hz b) Eigenmode 2, $f_2 = 3.3023$ Hz

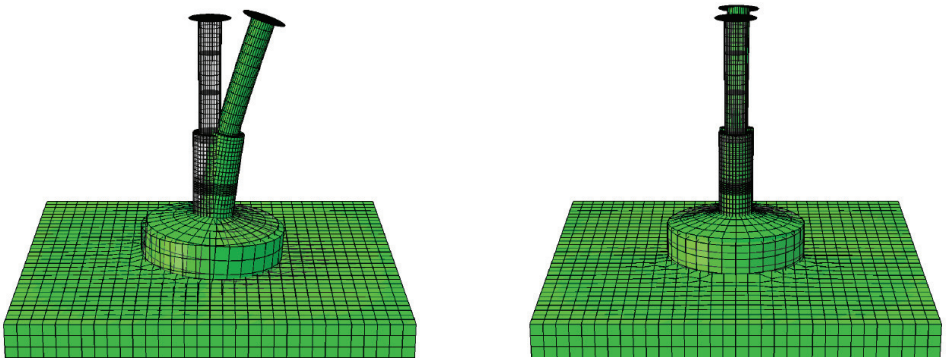

Figure 4.13: Flexible seabed, eigenmodes 1 and 2

Mode 3 and 4 are identical as well. As for mode 1 and 2 the modes involve a tilting of the tower, but in addition the tower is displaced along the seabed. Both modes have a modal amplitude of $\phi_3 = \phi_4 = 0.1146$ and a fundamental frequency of $f_3 = f_4 = 5.4399$ Hz.

a) Eigenmode 3, $f_3 = 5.4399$ Hz b) Eigenmode 4, $f_4 = 5.4399$ Hz

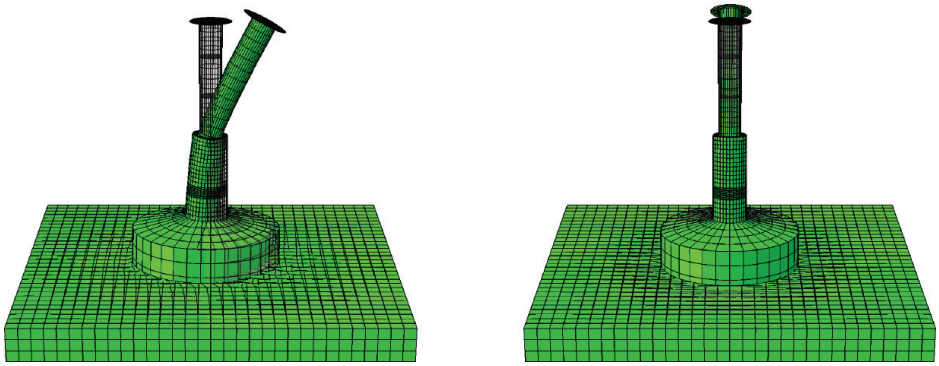

Figure 4.14: Flexible seabed, eigenmodes 3 and 4

Eigenmodes 5 and 6 involve a heavy distortion of the seabed and large deformations of the central tower. They have identical fundamental frequencies, $f_5 = f_6 = 8.4230$ Hz. Modal amplitudes are $\phi_5 = 0.1989$ and $\phi_6 = 0.1990$.

a) Eigenmode 5, $f_5 = 8.4230$ Hz

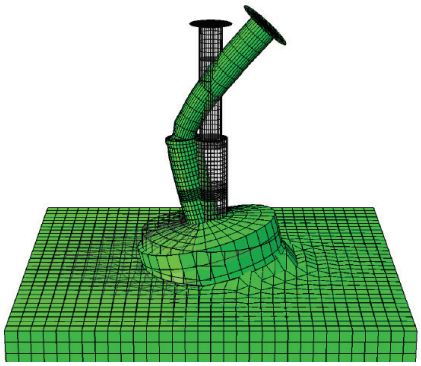

b) Eigenmode 6, $f_6 = 8.4230$ Hz

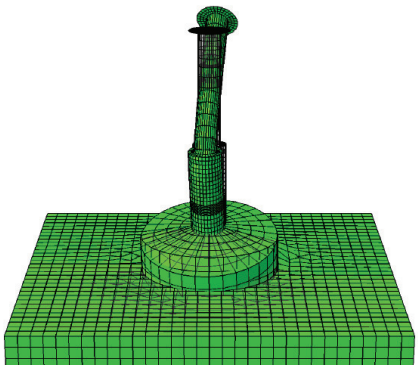

Figure 4.15: Flexible seabed, eigenmodes 5 and 6

Modes 7 and 8 have fundamental frequencies of $f_7 = f_8 = 10.931$ Hz. The modes are nearly identical and similar to mode 5 and 6, but the seabed is much less distorted. Modal amplitudes are $\phi_7 = 0.3303$ and $\phi_8 = 0.3607$.

a) Eigenmode 7, $f_7 = 10.931$ Hz

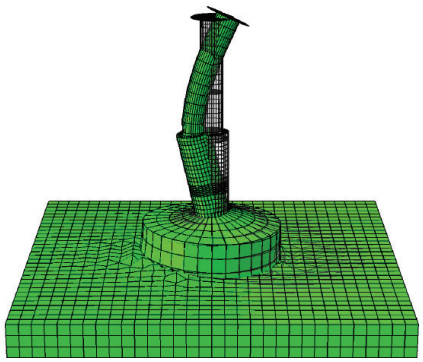

b) Eigenmode 8, $f_8 = 10.931$ Hz

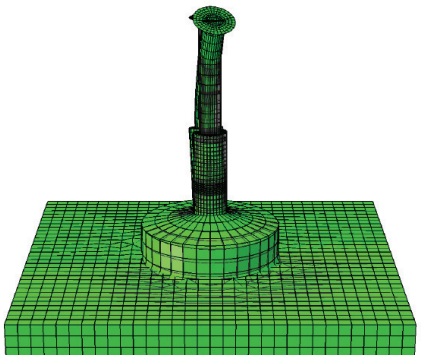

Figure 4.16: Flexible seabed, eigenmodes 7 and 8

In modes 9 and 10, the base of the tower is rotated. The modes have a fundamental frequency of $f_9 = f_{10} = 13.735$ Hz, and very little dispacement at waterlevel. The modal amplitudes of the modes are $\phi_9 = \phi_{10} = 0.0329$.

a) Eigenmode 9, $f_9 = 13.735$ Hz b) Eigenmode 10, $f_{10} = 13.735$ Hz

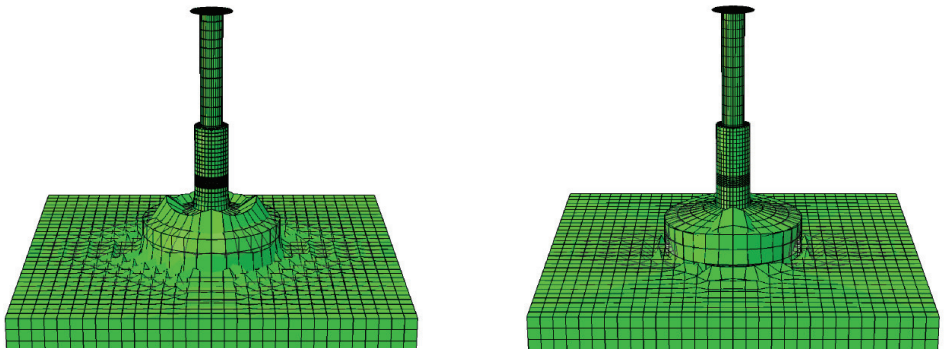

Figure 4.17: Flexible seabed, eigenmodes 9 and 10

Relevant data for dynamic analysis for the ten lowest structural eigenmodes are presented in Table 4.3. The data collected from the modal analysis has been used in the dynamic analysis.

Table 4.3: Frequency, generalized mass and modal amplitude, FSC discretization

Eigenmode	Frequency [rad/sec]	Frequency [1/sec]	Modal amplitude, ϕ_n	Generalized mass
1	20.749	3.3023	0.2185	35100
2	20.749	3.3023	0.2185	35100
3	34.180	5.4399	0.1146	50051
4	34.180	5.4399	0.1146	50051
5	52.923	8.4230	0.1989	51722
6	52.923	8.4230	0.1990	51722
7	68.682	10.931	0.3303	$1.80 \cdot 10^5$
8	68.682	10.931	0.3607	$2.80 \cdot 10^5$
9	86.303	13.735	0.0329	$1.64 \cdot 10^5$
10	86.303	13.735	0.0329	$1.64 \cdot 10^5$

4.4 Dynamic Analysis

4.4.1 Determination of dynamic properties

The eigenmodes which are of interest when performing a dynamic analysis are structural eigenmodes. Two eigenmodes which typically needs to be ivestigated for self excited vibrations are shown in Figure 4.18.

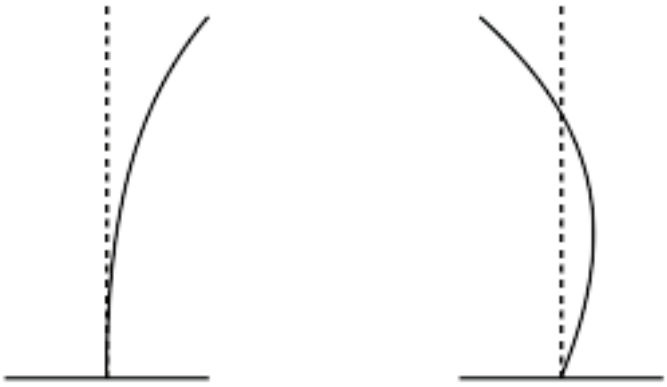

Figure 4.18: Eigenmodes most susceptible to dynamic amplification

From the results presented in Table 4.3, modal mass, stiffness and damping can be found using Eq. (3.18), (3.19) and (3.20). In Table 4.4 modal properties for the first fundamental modes are presented. Only unique modes are included, e.g. mode 1 and mode 2 are identical and only presented in the table as "Eigenmode 1".

Table 4.4: Modal mass, stiffness and stability criterion for a corresponding SDOF-system

Eigenmode	Frequency [1/sec]	M	C	K
1	3.3023	$7.3520 \cdot 10^5$	$3.0518 \cdot 10^7 \cdot \xi$	$3.1652 \cdot 10^8$
3	5.4399	$3.8110 \cdot 10^6$	$2.6052 \cdot 10^8 \cdot \xi$	$4.4523 \cdot 10^9$
5	8.4230	$1.3074 \cdot 10^6$	$1.3833 \cdot 10^8 \cdot \xi$	$3.6592 \cdot 10^9$
7	10.931	$1.6499 \cdot 10^6$	$2.2664 \cdot 10^8 \cdot \xi$	$7.7828 \cdot 10^9$
8	10.931	$2.1593 \cdot 10^6$	$2.9661 \cdot 10^8 \cdot \xi$	$1.0186 \cdot 10^{10}$
9	13.735	$1.5151 \cdot 10^8$	$2.6150 \cdot 10^10 \cdot \xi$	$1.1284 \cdot 10^{12}$

The stability criterion from the ISO-code, given by Eq. (3.25) and the velocity at the load point,

given by Eq. (3.27) are presented in Table 4.5. The stability criterion is used to evaluate a fundamental mode's susceptibility to self-excited vibrations. The first eigenmode has the lowest fundamental frequency, and also requires the highest ξ to ensure dynamic stability. Focus in the dynamic analysis will therefore be on this mode.

Table 4.5: Stability and velocity at loading point for the six first unique eigenmodes

Eigenmode	Frequency [1/sec]	Stability Criterion ξ_n	v_t [m/s]
1	3.3023	0.0626	0.1981
3	5.4399	0.0020	0.3264
5	8.4230	0.0114	0.5054
7	10.931	0.0193	0.6559
8	10.931	0.0175	0.6559
9	13.735	$1.6556 \cdot 10^{-6}$	0.8241

4.4.2 Sawtooth force function

Amplitude

The ISO-code and the recomendations provided by Kärnä (2006) gives two different approaches for determining the amplitude for use in a sawtooth force function. Figure 4.19 shows how the amplitude fraction, q, of the sawtooth force function varies with different damping coefficients. Eq. (3.26) has been used to calculate the amplitude fraction for use in correlation with the ISO-code. Scaling has been done using the ice velocity for mode 1, given in Table 4.4. Amplitude fraction as laid down by Kärnä has been calculated using Eq. (3.35).

The amplitude fraction of the force functions varies linearly with ξ according to both the ISO-code and the recommendations given by Kärnä. For a damping coefficient of $\xi = 0.02$, the ISO-code predicts an amplitude fraction of $q = 0.1222$. Kärnä's method yields an amplitude fraction of $q = 0.0860$ for the same damping coefficient.

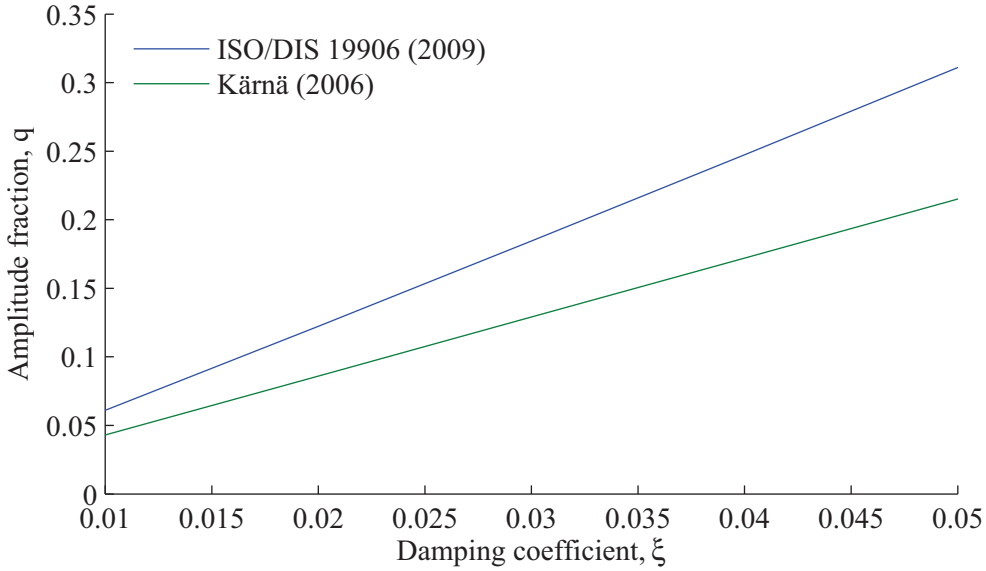

Figure 4.19: Damping ratio, ξ, plotted against amplitude fraction, q

ISO/DIS

The force function stated in the ISO-code is given as a sawtooth function where the maximum value, $F_{max} = F_{G,ISO}$. Amplitude, ΔF, is calculated using Eq. (3.26). Using an ice thickness of 1 m, an amplitude fraction of $q = 0.1222$ the amplitude becomes:

$$\Delta F_{ISO} = 0.1222 \cdot 4.40 \cdot 10^6 = 5.3768 \cdot 10^5$$

The amplitude is then used in the dynamic force function. With a fundamental frequency of $f = 3.3032$ Hz, Eq. (3.28) gives the force function:

$$F_{dyn,ISO} = 4.40 \cdot 10^6 + 2.6885 \cdot 10^5 \cdot (\text{sawtooth}(2\pi \cdot 3.3032t) - 1)$$

$F_{dyn,ISO}$ and the displacement plotted against time is shown in Figure 4.20. The displacement, u, has been determined using Newmark's method, given in Eq. (3.21) and (3.22). Figure 4.21 shows how the dynamic amplification factor, DAF, varies with different damping factors. Because lower damping fractions leads to lower amplitude fractions, the variation of Björnklacken's DAF is minimal.

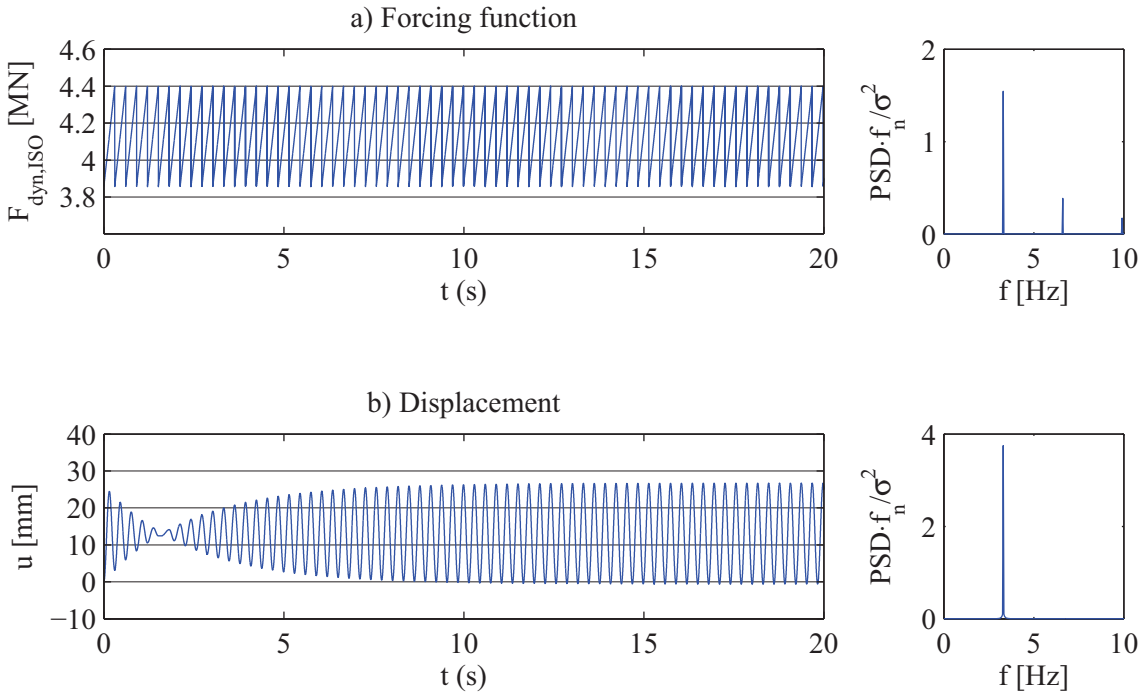

Figure 4.20: Forcing function, displacement and velocity for a sawtooth function, where $\xi = 0.02$ and $q = 0.1235$

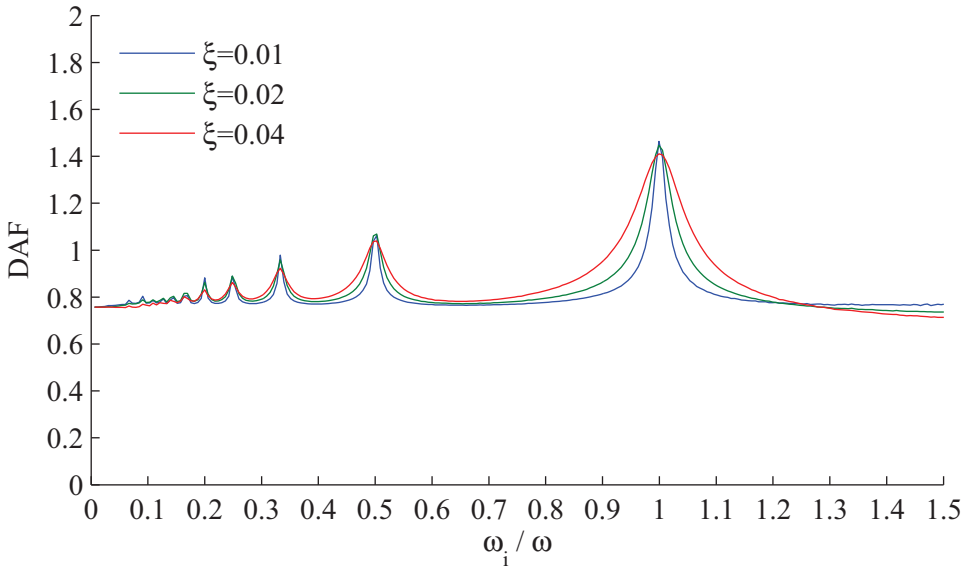

Figure 4.21: DAF for a sawtooth function where $q = 0.1235$

Kärnä (2006)

Except for a corrected amplitude fraction, the sawtooth force function according to Kärnä (2006) is identical to the function proposed in the ISO-code. The amplitude fraction if the damping fraction is $\xi = 0.02$ becomes $q = 0.0860$. If the ice thickness is 1 m, the amplitude is given as:

$$\Delta F_{Kärnä} = 0.0860 \cdot 4.40 \cdot 10^6 = 3.7840 \cdot 10^5$$

Implemented in Eq. (3.28), the force function for the first eigenmode then becomes:

$$F_{dyn,Kärnä} = 4.40 \cdot 10^6 + 1.8920 \cdot 10^5 \cdot (\text{sawtooth}(2\pi \cdot 3.3032t) - 1)$$

Figure 4.22 shows the force function and displacement when $F_{dyn,Kärnä}$ has been applied to the SDOF-system. Similar to what analyses performed where q has been scaled in accordance with the ISO-code shows, the damping fraction has little influence on the DAF in Björnklacken's case.

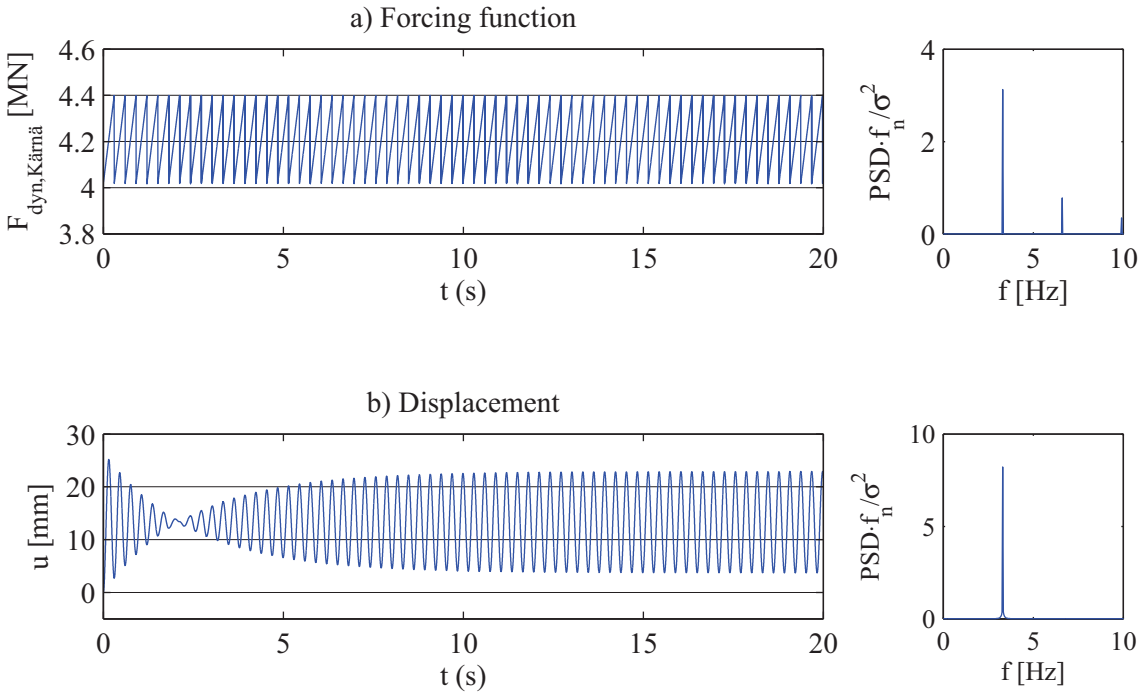

Figure 4.22: Forcing function, displacement and velocity for a sawtooth function, where $\xi = 0.02$, and $q = 0.0868$

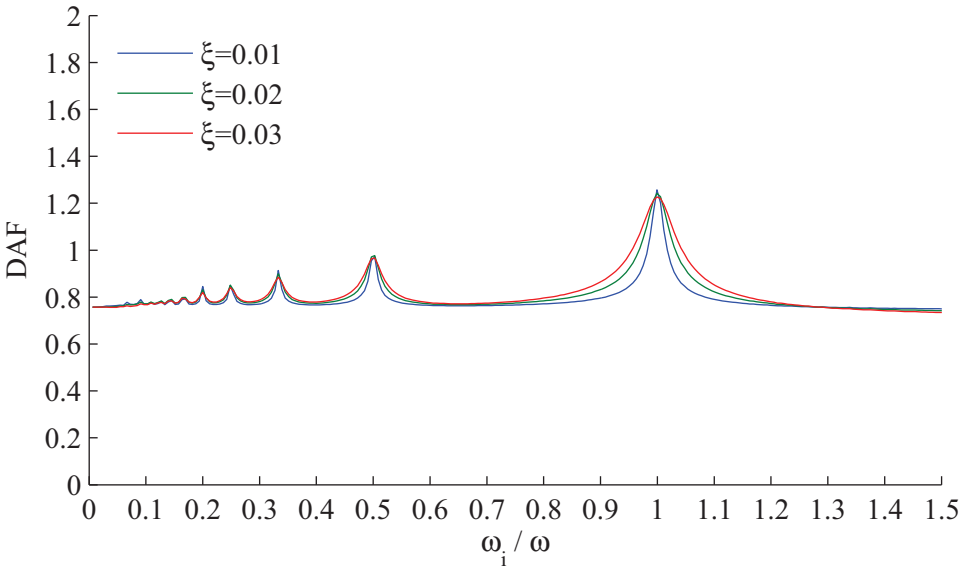

Figure 4.23: DAF for a sawtooth function where $q = 0.0868$

4.4.3 IEC

Dynamic loading according to the method proposed in the IEC-code is a sinusoidal force function, given in Eq. (3.30). Using the static load from the static analysis as the static force component, with ice thickness $h = 1$ m and $f = 3.3032$ Hz, the dynamic force function becomes:

$$F_{dyn,IEC} = 6.46 \cdot 10^6 \cdot \left(\frac{3}{4} + \frac{1}{4} sin(2\pi \cdot 3.3032t \right)$$

The force function and corresponding displacements are shown in Figure 4.24. A damping fraction of $\xi = 0.02$ has been used in the analysis, and displacement has been calculated using Newmark's method, given in Eq. (3.21) and (3.22). The dynamic amplification factor for $\xi = 0.01$, $\xi = 0.02$ and $\xi = 0.03$ is shown in Figure 4.25. For a damping fraction of $\xi = 0.01$, the dynamic amplification factor exceeds $DAF = 14$.

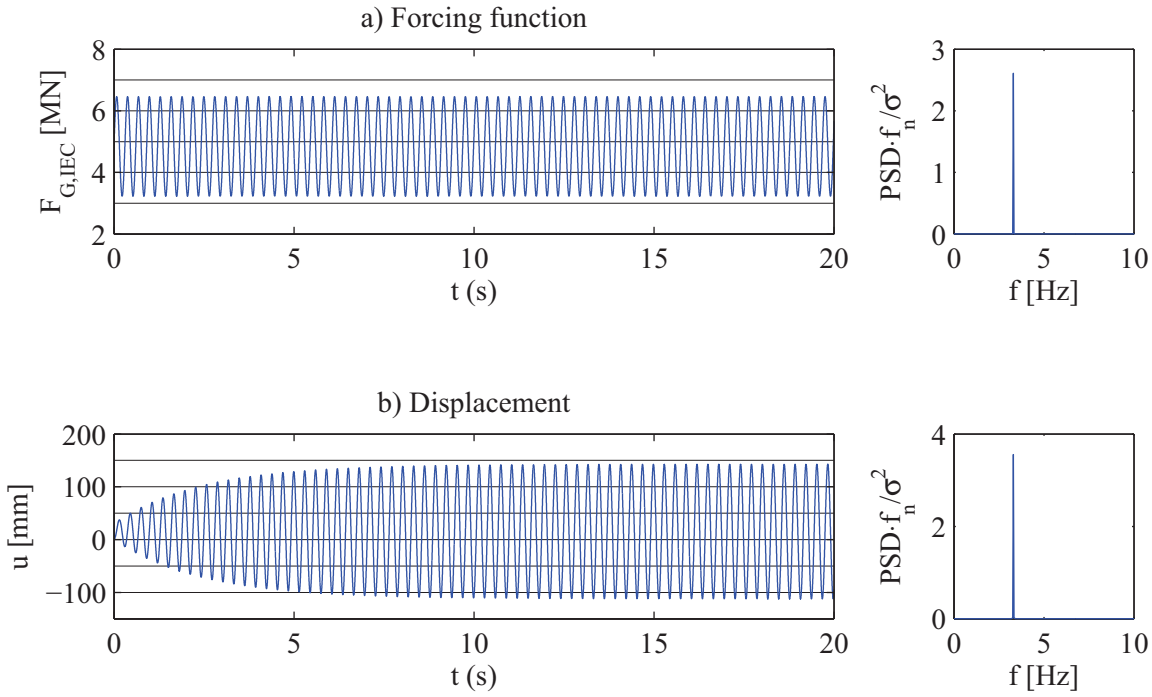

Figure 4.24: Forcing function, displacement and velocity for a harmonic forcing function where $\xi = 0.02$

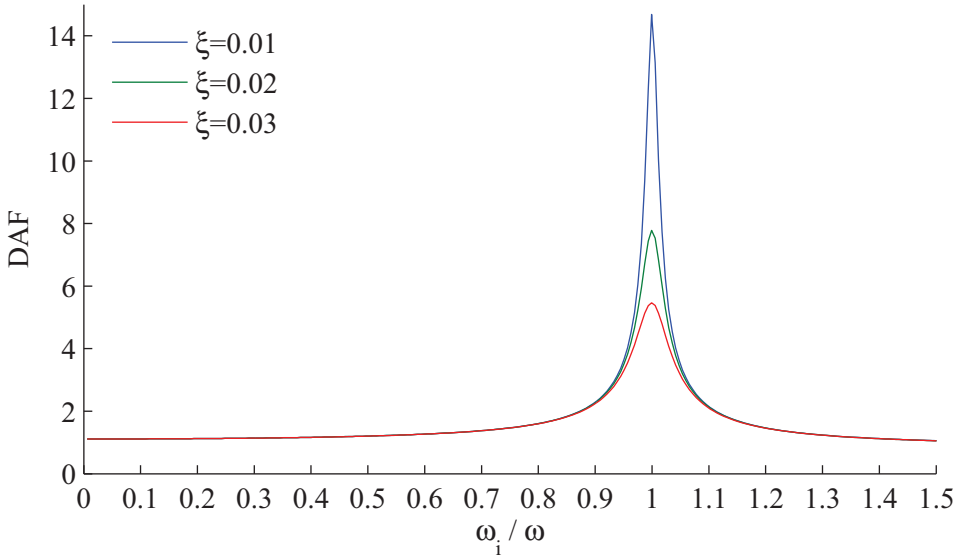

Figure 4.25: DAF for a harmonic force function with varying ξ

4.4.4 Comparison

Figure 4.26 shows DAF at different damping coefficients for dynamic loading calculated using forcing functions from the IEC- and the ISO-code. Because of the velocity scaling at load point, the sawtooth function is almost not influenced by the damping coefficient for the ISO-code and for the results acquired using Kärnä' method (2006). In comparison, a sawtooth function where the velocity has not been scaled and a harmonic forcing function predicts very high dynamic amplification factors for low damping fractions.

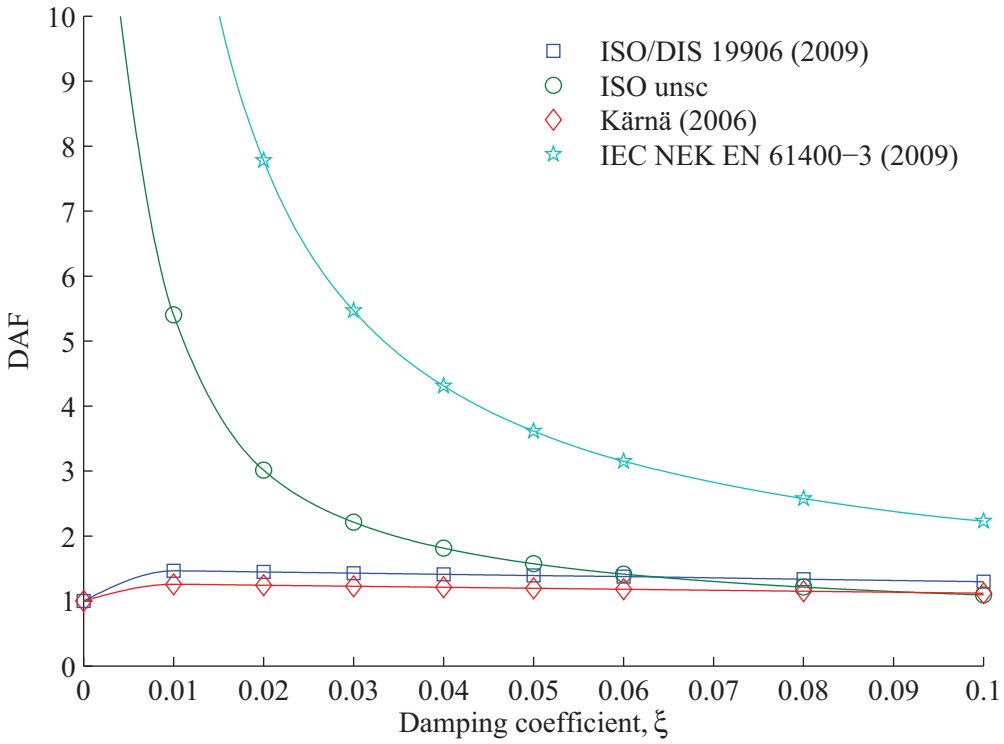

Figure 4.26: DAF plotted against damping coefficient

Figure 4.27 shows how the DAF varies with different frequencies, expressed as fractions of the fundamental frequency, ω_i. The dotted line shows a limit value proposed by Kärnä et. al. (2006). Structures with dynamic amplification factors higher than this value may experience self-excited vibrations, and should be examined closer for dynamic effects. All of the dynamic forcing functions predict a DAF higher than 1.2 if the forcing function is applied in the same frequency as the structure's fundamental mode.

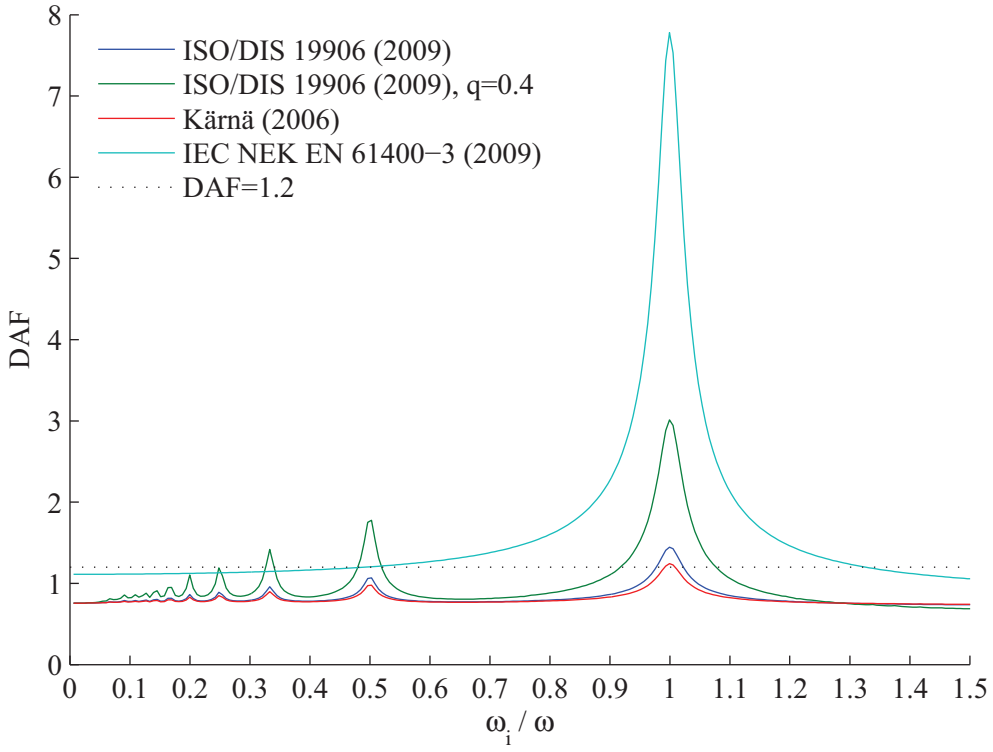

Figure 4.27: DAF for ISO/DIS and IEC with $\xi = 0.02$

5 Discussion

5.1 Numerical modelling

Björnklacken

The model of Björnklacken used in this work is based on sketches presented by Engelbrektsson (1987). No accurate construction drawings have been available. Weight calculations based on standard densities for reinforced conrete, differed from calculations made by Engelbrektsson (1987) by 5%. The reasons for the dissimilarity are unknown. Since neither Engelbrektsson's calculations or the material properties used are detailed, the weight found in the current work has been used in the analyses.

Frequencies, generalised mass and stiffness were found from modal analyses. The lowest fundamental frequency found was 3.30 Hz. No recordings of frequencies was available for Björnklacken, but recordings exists for similar structures. Fundamental frequencies of 2.6 Hz for the lighthouse Norströmsgrund (Engelbrektson 1989) and 0.9 Hz for the Kemi I lighthouse (Määttänen 1975) has been reported. Compared to these measurements, Björnklacken's fundamental frequency seems a little high. However, Björnklacken is considerably smaller than both Norströmsgrund and Kemi I and this could be an explanation for the difference in frequencies. In addition to Björnklacken's small size only a small percentage of Björnklacken's weight lies above the waterline. This means that much of Björnklacken's mass is not included in the lowest eigenmode. Generalised mass and stiffness for Björnklacken are also lower than what has been reported for similar structures (Kärnä 2006).

Elements and materials

Shell elements are favourable compared to solid elements in terms of analysis running time, and generally provide accurate results for analysis where the elements have a low thickness to span ratio. For these reasons the majority of the structure was modelled using shell elements, as shown in Figure 3.5. The thick base of the lighthouse with a dense mesh in the centre was

discretizised using solid elements, due to a high thickness to span ratio. Solid elements were also used to model the transition between the lower and upper central tower. The transition had a high thickness to span ratio, but could probably have been simplified using shell elements without affecting global action in any noteworthy degree.

The iron ore filling documented by Engelbrektson (1987) was discretizised as an increase in the density of the central tower and the lighthouse base elements. Contributions the iron ore would have to the global stiffness, have thus been ignored for the purpose of static and modal analysis. Local contributions to stiffness has been implemented in the numerical model by increasing the material stiffness in the section where the load was applied. Another way to model the iron ore filling is to use solid elements. This option was not investigated in this project, since a large solid element within the tower would mean implementing new interaction and material properties. Ill-defined interaction and material properties could lead to an unwanted increase in stiffness. Without any prior knowledge on the subject, and without measurements from Björnklacken, these properties would be hard to define without influencing the structure's behaviour. Therefore, the simplified method where equivalent densities have been introduced has been used in the current work.

Seabed modelling

The seabed was modelled as a solid element with varying stiffness over depth. Since no test data from the area around Björnklacken was available, the stiffness was based on recommendations from geotechnical experts at NTNU (Nordahl 2010). Figure 3.8 shows how the density of the soil varies, from 80 MPa where the seabed is in contact with the lighthouse to 160 MPa 24 m below the seabed. Because of the lack of measurements for Björnklacken, the seabed's behaviour during analysis is hard to verify.

The three different models for soil-structure interaction, shown in Figure 3.7, reacted very different to applied loads. The FB model, which can basically be regarded as a cantilever beam of varying stiffness, acted very stiff. A reference static load of 4.40 MN resulted in a displacement at waterline of only 1.80 mm. In contrast to this, an identical load caused the FSU model to start tilting and lose contact with the seabed. A static load of 4.40 MN resulted in a displacement at waterline of 18.35 mm. At higher loads the difference between the two models grows, as second order effects causes the FSU model to tilt even faster. The FSC model acted very similar to the FSU model at lower loads, but acted stiffer at higher loads because of it's constraint.

Because of the prestressed rock-anchors installed in the winter 1970 (Engelbrektsson 1987), the actual behaviour of Björnklacken is assumed to be most similar to the FSC model. The rock-

anchors were installed to prevent lateral displacement, but they also prevented Björnklacken from losing contact with the seabed. This prevented second-order effects, and made a contribution to Björnklacken's resistance to overturning. After the rock-anchors broke, Björnklacken was displaced laterally. This leads to the assessement that the FSC model should be used for simulating Björnklacken's behaviour pre-failure, while the FSU model should be used for simulating it's behaviour after the rock-anchors failed.

5.2 Ambient Conditions

Ice conditions

The actual ice thickness at the time of failure is uncertain. Engelbrektsson (1987) reported an ice thickness of as much as 1.4-1.5 m around the lighthouse. SMHI's ice charts (Lind 2010) show a general ice thickness of around 0.6-0.8 m in the area. In comparison, Eq. (3.3), proposed by Zubov (1943), suggests an ice thickness of 0.93 m. Zubov's equation is based on observations, and has proven to be a good indicator for ice thickness (Bjerkås 2010).

Previous experiences have shown that ice thickness in general is lower around structures in ice (Bjerkås 2010). Based on this, the measurements made by Engelbrektson (1987) seems too high. The build-up of ice ridges can also take place when an ice floe comes to rest against a structure (ISO/DIS 19906 2009), as was the case in the winter of 1984/85. Experiences show, however, that build-up of low-density rubble ice will not necessarily correspond to an equal increase in effective ice-thickness (Bjerkås 2010). SMHI's ice charts only shows general ice thickness in an area, and only give approximate values. Therefore, Zubov's equation has been used for the purpose of estimating ice thickness in this report, with a predicted ice thickness of approx. 0.93 m the 4th of April 1985.

Special considerations

In the report from Engelbrektson (1987), an observation of a large ice floe that enclosed the lighthouse is mentioned. High wind speeds in the period when Björnklacken's rock anchors broke was also reported, and it was further proposed that the high wind speed caused rapid ice movement. The ice floe and the rapid ice movement may have been contributing causes to Björnklacken's failure, but is difficult to simulate since exact data for both wind speed and the ice floe is lacking.

5.3 Static loads

Collapse moment

The force required to break the rock anchors is assumed to be 13.83 MN, as estimated in Subsection 4.2.3. This force can be considered reliable, based on the results from Engelbrektsson (1987). All methods of estimating static ice load, except the formula from the API-code (2009), requires an ice thickness much larger than 1 m to predict a load of this magnitude.

Engelbrektson (1987) reports an interesting observation: For the time period up to 1987, larger structures withstood ice forces without significant damage except for some abrasion and minor vibration effect. Meanwhile, several smaller structures were damaged and even destroyed. Several small Finnish lighthouses with a diameter of approximately 1 m, and Swedish lighthouses with diameter between 2.5 m and 3 m were damaged. Lighthouses built in that time period were designed using Eq. (3.33) according to a load which is linearly dependent on the diameter of the structure. Engelbrektson's findings can signify that either smaller structures are more susceptible to self-excited vibrations, or that static pressure increases with smaller diameter. One approach where the pressure increases with a lower diameter is the method given in the API-code, shown in Eq. (3.31). Figure 4.4 a) shows that the method given in the API-code is the only one which predicts a static load high enough for failure.

Lateral displacement

After the tendons collapsed, the lighthouse was displaced approximately 17 m along the seabed, before it came to rest in an inclined position. This means that the ice loads must have exceded the limit force dependent on the friction between the seabed and the base of the lighthouse. According to the results presented in Figure 4.7, lateral displacement would occur when the ice thickness reaches 0.45 m according to the IEC-code, and 0.5 m according to the ISO-code. The lateral displacement can therefore be explained as a result of static ice loading alone, since the ice thickness in the winter of 1984/85 was well above 0.5 m, independent of which method is used.

An overview of the ice thickness each year for the time period 1965-1995, based on the equation proposed by Zubov (1943), is shown in Figure 4.2. It is worth noticing that the ice thickness in 1969/70 (0.91m) is sufficient according to both the ISO- and the IEC-code to predict lateral displacement, if a CoF of 0.45 is used. This is in accordance with the observations made during the winter of 1970, when a lateral displacement of approx 10 cm was reported (Björk 1981).

5.4 Modal Analysis

In the modal analysis performed in ABAQUS/CAE, the seabed has been taken as the slave surface (Hibbit et. al. 2008). This enables the nodes of the lighthouse to penetrate the surface of the seabed. Normally, the surface with the most dense mesh should be defined as the slave surface. It could be argued that the choice of master-slave surfaces makes the results unreliable. Due to the dense mesh of both the seabed and the lighthouse, and the behaviour of soils, this has been neglected in the current work. Analyses carried out where the seabed has been set as the master surface, meaning that no penetration of the seabed can occur, showed a higher fundamental frequency.

5.5 Dynamic Responce

In the dynamic analyses where sawtooth forcing functions were applied, the stability coefficient, θ, suggested by the ISO-code was used. Other work has shown that an appropriate value for θ needs to be estimated for wide or compliant structures. Bjerkaas (2009) reported that vibrations occured on Norströmsgrund lighthouse with an ice thickness of 0.7 m. Lønøy (2010) proposed that if the damping ratio is known for the structure, the stability coefficient can be calculated using Eq. (3.25). Assuming a damping ratio of $\xi = 0.02$, Lønøy showed that a value for the stability coefficient should have been between $100 \cdot 10^6$ and $120 \cdot 10^6$ in Norströmsgrund's case. Since no measurements of fundamental frequencies or damping ratio exists for Björnklacken lighthouse, the stability coefficient recommended by the ISO-code has been used in the current work.

Scaling of the amplitude, as proposed in the ISO-code and by Kärnä (2006), leads to an increase in q when more damping is applied to the SDOF-system. This is shown in Figure 4.19, where q is shown to be linearily related to ξ. Eq. (3.35) shows how the amplitude is dependent on the stiffness of the structure. The eigenmode of Björnklacken which is assumed to be most susceptible to self-excited vibrations, also has a very low stiffness.

Compared to calculations performed by Kärnä et. al. (2006), the stiffness of Björnklacken's lowest eigenmode is approximately 1/10 of the stiffness of Norströmsgrund's lowest mode. Since the amplitude is linearily dependent on the stiffness, a very low stiffness leads to a very low amplitude. In Björnklacken's case, this means that the velocity scaling influences the dynamic amplification caused by self-excited vibrations more than the damping fraction. When scaling of q proposed by Kärnä (2006) is applied to Björnklacken's lowest fundamental mode with

$\xi = 0.01$, the amplitude fraction is given as only $q = 0.0430$. This means that the amplitude is only 4.3 percent of the maximum force.

Kärnä et. al. (2006) recommended that a structure with a dynamic amplification factor higher than 1.2 can be expected to suffer from self-excited vibrations. As shown in Figure 4.27, all codes predicts dynamic effects exceeding this limit. This underlines the need for a full-scale dynamic analysis.

6 Conclusions and further work

6.1 Conclusions

The current work was carried out to determine the level of ice forces which caused the collapse of Björnklacken lighthouse the 4th of April 1985. Both static and dynamic ice action has been calculated in accordance with common design codes.

Data from SMHI show that while the winter of 1985 was cold, it was not exceptionally strong compared to some of the earlier years in Björnklacken's operation period. This leads to the conclusion that other factors, such as wind speed and the ice floe reported by Engelbrektson (1987), contributed to the overloading event.

The design ice load used in the time period Björnklacken was installed gave a linear relationship between structural diameter and load. Damages on structures subjected to ice forces has shown that a linear relationship between load and diameter tends to underestimate ice loads on smaller structures.

Ice loads calculated in accordance with common design codes includes a more sophisticated relationship between the shape of the structure and load. Only the API-code predicted static ice loads of a high enough magnitude to cause a collapse in the structure. However, both the IEC- and the ISO-code predicted displacements at waterline of such magnitude that dynamic analysis is recommended.

Modal analysis done on a numerical model of Björnklacken showed a fundamental frequency of approximately 3.30 Hz. A fundamental frequency of this magnitude is high, but since no measurements of vibration on Björnklacken exists, it was not possible to certify the frequency's authenticity.

Dynamic analysis of Björnklacken, simplified as a SDOF-system, showed large differences in dynamic responce dependent on which forcing function was used. Dynamic ice load represented by a harmonic forcing function caused more dynamic responce in the structure than a sawooth forcing function.

The amplitude of a sawtooth forcing function was significantly reduced if the amplitude fraction was scaled in accordance the with ISO-code. No similar guidelines exists in the IEC-code, meaning that the amplitude of the vibrations caused by harmonic functions are calculated independent of the ice-velocity. A recommendation would be that guidelines for amplitude scaling should be given in the IEC-code as well as the ISO-code.

Results from the dynamic analysis showed that Björnklacken lighthouse was likely to suffer from occasional self-excited vibrations. Based on these results, a full-scale dynamic analysis should be performed.

6.2 Further work

- The discretization of the seabed should be adressed. An analysis where results could be compared to measured data could help verify the properties of the seabed. This was not possible in Björnklacken's case, since no measurements of vibrations exists.
- Studies should be directed at determining how the large ice floe, reported by Engelbrektson (1987), influenced Björnklacken.
- Instead of simplifying the problem as a SDOF-system, more modes could be included in the analysis. Although higher modes show little susceptibility to self-induced vibrations, they could have an important influence on the results if combined with lower modes.
- A full-scale dynamic analysis should be performed using FEA-software.

References

Albreksten, A. (2009), *Prediction of the Responce from Ice Forces to a Lighthouse Structure*, Master Thesis, Norwegian University of Science and Technology, Trondheim

API RP-2N (1995), *Recommended Practice for Planning, Designing and Constructing Structures and Pipelines for Arctic Conditions*, American Petroleum Institute, 82 p.

Bjerkås, M. (2006), *Ice actions on offshore structures - with applications of continuous wavelet transforms on ice load signals*, PhD thesis, Norwegian University of Science and Technology, Trondheim

Bjerkås, M. (2010), Information and guidance (Personal communication, Spring 2010)

Björk , B. (1981), Ice-induced vibrations of fixed offshore structures, *Marine structures and ships in ice Report No 81-06/2*, Joint Norwegian research project, Norway

Chopra, A. K. (2007), *Dynamics of Structures - Theory and Applications to Earthquake Engineering (3rd Ed).* Pearson Prentice Hall, New Jersey

Engelbrektson, A. (1987), Evaluation of Extreme Ice forces on a Lighthouse in the Bothnian Bay: A study of the Björnklacken event in April 1985, *Ice forces against offshore structures report No. 1*, VBB, NASN and the University of Luleå, Sweden

Engelbrektson, A. (1989), An ice-structure interaction model based on observations in the Gulf of Bothnia. *Proc. 10th Int. Conf. Port and Ocean Eng. under Arctic Cond.*, Luleå, Sweden, June 12-16, Vol. 1. pp. 504-517.

Fransson, L. and Bergdahl, L. (2009), Recommendations for design of offshore foundations exposed to ice loads, *Elforsk rapport 09:55*, Elforsk, Sweden

IEC 61400-3:2009 (2009), *Design Requirements for Offshore Wind Turbines*, International Electrotechnical Commision. 2009-02.128 p.

ISO/DIS 19906 (2009), Arctic offshore structures, Draft International Standard. 2009-01-15. 428 p.

Hibbit, Karlsson and Sorensen (2008), ABAQUS Analysis User's Manual, *ABAQUS Documentation Collection,* Hibbit, Karlsson and Sorensen Inc., USA

Kärnä, T. (2006), How to use saw-tooth force functions to model self-excited vibration, *Report Nro. Karna-6-2006*, Karna Research and Consulting, Sweden

Kärnä, T., Qianjin, Y., Yan, Q. and Xiangjun, B. (2007), Ice force spectrum on narrow conical structures, *Cold Regions Science and Technology* [online], 49(2) Available from: linkinghub.elsevier.com/retrieve/pii/S0165232X07000237 [Downloaded 29. May 2010]

Kullenberg, G. (1981) Physical Oceanography. A. Voipio (Ed.), *The Baltic Sea: Elsevier Oceanography Series*, (Vol. 30, p. 135-181), Elsevier Scientific Publishing Company

Lehmann, T. Ø. (2010), *Prediction of the responce from ice forces on a lighthouse structure - Reevaluation of the Nygrån event*, Master thesis, Norwegian University of Science and Technology, Trondheim

Lønøy, C. (2010), *Application of Predefined Forcing Functions to Represent Dynamic Ice Actions*, Norwegian University of Science and Technology, Trondheim

Määttänen, M. (1975), Experiences of ice forces against a steel lighthouse mounted on the seabed, and proposed constructional refinements. *Proc. 3rd Int. Conf. Port and Ocean Eng. under Arctic Cond.*, Fairbanks, Alaska, 11-15 August 1975, Vol II, pp. 857-869.

Nordahl (2010), personal communication, Spring 2010

NS3473 (2003), *Concrete structures - Design and detailing rules*, Standard Norge, 78 p.

Russel, A. (2010), Coefficient of friction for a gravity based structure [E-mail] (Personal communication, 25. February 2010)

Lind, L. (2010), Istykkelse nær Björnklacken fyrtårn (In Norwegian) [E-mail] (Personal communication, 5. March 2010)

Sodhi, D.S. (1988), Ice-induced vibrations of structures, IAHR Ice Symposium, Vol. 3, pp. 625-657.

USGS World Assessment Team (2000), U.S. Geological Survey World Petroleum Assessment 2000 - Description and Results: *U.S. Geological Survey Digital Data Series - DDS60* [Online], Available from: http://pubs.usgs.gov/dds/dds-060/ [Downloaded 29. May 2010]

APPENDIX A: INPUT FILE

```
*HEADING
BJORNKLACKEN LIGHTHOUSE
**
*PREPRINT, ECHO=YES, HISTORY=YES, MODEL=YES
**
*RESTART, WRITE, FREQ=1
**
*FILE FORMAT, ZERO INCREMENT
**
*PART, NAME=LIGHTHOUSE
**
***************
**TOWER_PT1**
***************
**
**Below intersection - cone/tower
**
*NODE
11100,   0.0,       0.0,       0.5
11101,   1.45,      0.0,       0.5
11109,   0.0,       1.45,      0.5
11117,   -1.45,     0.0,       0.5
11125,   0.0,       -1.45,     0.5
**
*NGEN, LINE=C, NSET=TOWER_PT1_LOWER
11101, 11109, 1, 11100
11109, 11117, 1, 11100
11117, 11125, 1, 11100
11125, 11101, 3, 11100
**
*NCOPY, old set=TOWER_PT1_LOWER, newset=TOWER_PT1_MID, change number=1000, shift
0,0,4.00
0,0,0
**
*NFILL, NSET=TOWER_PT1_NODES
TOWER_PT1_LOWER, TOWER_PT1_MID, 5, 200
**
*ELEMENT, TYPE=S4R
11001, 11101, 11102, 11302, 11301
11025, 11125, 11128, 11328, 11325
11032, 11146, 11101, 11301, 11346
**
*ELGEN, ELSET=TOWER_PT1
11001, 24, 1, 1, 5, 200, 100
11025, 7, 3, 1, 5, 200, 100
11032, 1, 1, 1, 5, 200, 100
**
**Above intersection
**
*NCOPY, old set=TOWER_PT1_MID, newset=TOWER_PT1_UPPER, change number=1000, shift
0,0,1.400
0,0,0
**
*NFILL, NSET=TOWER_PT1
TOWER_PT1_MID, TOWER_PT1_UPPER, 5, 200
**
*ELEMENT, TYPE=S4R
12001, 12101, 12102, 12302, 12301
12025, 12125, 12128, 12328, 12325
12032, 12146, 12101, 12301, 12346
```

```
**
*ELGEN, ELSET=TOWER_PT1
12001, 24, 1, 1, 5, 200, 100
12025, 7, 3, 1, 5, 200, 100
12032, 1, 1, 1, 5, 200, 100
**
***************
**TOWER_PT2**
***************
**
**The refined section
**
*NCOPY, old set=TOWER_PT1_UPPER, newset=TOWER_PT2_UPPER, change number=1000, shift
0,0,1.000
0,0,0
**
*NFILL, NSET=TOWER_PT2_NODES
TOWER_PT1_UPPER, TOWER_PT2_UPPER, 10, 100
**
*ELEMENT, TYPE=S4R
13001, 13101, 13102, 13202, 13201
13025, 13125, 13128, 13228, 13225
13032, 13146, 13101, 13201, 13246
**
*ELGEN, ELSET=TOWER_PT2
13001, 24, 1, 1, 10, 100, 100
13025, 7, 3, 1, 10, 100, 100
13032, 1, 1, 1, 10, 100, 100
**
***************
**TOWER_PT3**
***************
**
**Above the waterline
**
*NCOPY, old set=TOWER_PT2_UPPER, newset=TOWER_PT3_UPPER, change number=1000, shift
0,0,3.700
0,0,0
**
*NFILL, NSET=TOWER_PT3_NODES
TOWER_PT2_UPPER, TOWER_PT3_UPPER, 10, 100
**
*ELEMENT, TYPE=S4R
14001, 14101, 14102, 14202, 14201
14025, 14125, 14128, 14228, 14225
14032, 14146, 14101, 14201, 14246
**
*ELGEN, ELSET=TOWER_PT3
14001, 24, 1, 1, 10, 100, 100
14025, 7, 3, 1, 10, 100, 100
14032, 1, 1, 1, 10, 100, 100
**
****************
**TOWER_BASE**
****************
**
*NODE
1100,    0.0,      0.0,      0
1101,    6,        0.0,      0
1109,    0.0,      6,        0
```

```
1117,    -6,       0.0,      0
1125,    0.0,      -6,       0
1401,    2.55,     0.0,      0
1409,    0.0,      2.55,     0
1417,    -2.55,    0.0,      0
1425,    0.0,      -2.55,    0
1501,    1.45,     0.0,      0
1509,    0.0,      1.45,     0
1517,    -1.45,    0.0,      0
1525,    0.0,      -1.45,    0
**
*NGEN, LINE=C, NSET=OUTER_BASE_O_L
1101, 1109, 1, 1100
1109, 1117, 1, 1100
1117, 1125, 1, 1100
1125, 1101, 3, 1100
*NGEN, LINE=C, NSET=OUTER_BASE_M_L
1401, 1409, 1, 1100
1409, 1417, 1, 1100
1417, 1425, 1, 1100
1425, 1401, 3, 1100
*NGEN, LINE=C, NSET=OUTER_BASE_I_L
1501, 1509, 1, 1100
1509, 1517, 1, 1100
1517, 1525, 1, 1100
1525, 1501, 3, 1100
**
*NCOPY, old set=OUTER_BASE_O_L, newset=OUTER_BASE_O_U, change number=1000, shift
0,0,0.500
0,0,0
**
*NCOPY, old set=OUTER_BASE_M_L, newset=OUTER_BASE_M_U, change number=1000, shift
0,0,0.500
0,0,0
**
*NFILL, NSET=OUTER_BASE_BOTTOM
OUTER_BASE_O_L, OUTER_BASE_M_L, 3, 100
*NFILL
OUTER_BASE_O_U, OUTER_BASE_M_U, 3, 100
**
*ELEMENT, TYPE=C3D8R
1001, 1101, 1102, 1202, 1201, 2101, 2102, 2202, 2201
1025, 1125, 1128, 1228, 1225, 2125, 2128, 2228, 2225
1032, 1146, 1101, 1201, 1246, 2146, 2101, 2201, 2246
1401, 1401, 1402, 1502, 1501, 2401, 2402, 11102, 11101
1425, 1425, 1428, 1528, 1525, 2425, 2428, 11128, 11125
1432, 1446, 1401, 1501, 1546, 2446, 2401, 11101, 11146
**
*ELGEN, ELSET=OUTER_BASE
1001, 24, 1, 1, 1, 1000, 100, 3, 100, 100
1025, 7, 3, 1, 1, 1000, 100, 3, 100, 100
1032, 1, 1, 1, 1, 1000, 100, 3, 100, 100
1401, 24, 1, 1, 1, 1000, 100
1425, 7, 3, 1, 1, 1000, 100
1432, 1, 1, 1, 1, 1000, 100
**
*NODE
90101,   0.900,   -0.900,   0
90105,   0,       -1.16,    0
90109,   -0.900,  -0.900,   0
```

```
90501,   1.16,     0,        0
90505,   0,        0,        0
90509,   -1.16,    0,        0
90901,   0.900,    0.900,    0
90905,   0,        1.16,     0
90909,   -0.900,   0.900,    0
**
*NGEN, NSET=INNER_BASE_lower
90101,   90105,   1
90105,   90109,   1
*NGEN, NSET=INNER_BASE_middle
90501,   90505,   1
90505,   90509,   1
*NGEN, NSET=INNER_BASE_upper
90901,   90905,   1
90905,   90909,   1
**
*NFILL, NSET=INNER_BASE_1
INNER_BASE_lower, INNER_BASE_middle, 4, 100
INNER_BASE_middle, INNER_BASE_upper, 4, 100
**
*NCOPY, old set=INNER_BASE_1, new set=INNER_BASE_2, change number=1000, shift
0,        0,        0.500

*ELEMENT, TYPE=c3d8r
90101, 90101, 90201, 90202, 90102, 91101, 91201, 91202, 91102
**
*ELGEN, ELSET=INNER_BASE
90101, 8, 100, 100, 8, 1, 1
**
*ELEMENT, TYPE=c3d8r, ELSET=INNER_BASE
91101,   90101,   1537,    1540,    90201,   91101,   11137,   11140,   91201
91201,   90201,   1540,    1543,    90301,   91201,   11140,   11143,   91301
91301,   90301,   1543,    1546,    90401,   91301,   11143,   11146,   91401
91401,   90401,   1546,    1501,    90501,   91401,   11146,   11101,   91501
91501,   90501,   1501,    1502,    90601,   91501,   11101,   11102,   91601
91601,   90601,   1502,    1503,    90701,   91601,   11102,   11103,   91701
91701,   90701,   1503,    1504,    90801,   91701,   11103,   11104,   91801
91801,   90801,   1504,    1505,    90901,   91801,   11104,   11105,   91901
91102,   1521,    90109,   90209,   1520,    11121,   91109,   91209,   11120
91202,   1520,    90209,   90309,   1519,    11120,   91209,   91309,   11119
91302,   1519,    90309,   90409,   1518,    11119,   91309,   91409,   11118
91402,   1518,    90409,   90509,   1517,    11118,   91409,   91509,   11117
91502,   1517,    90509,   90609,   1516,    11117,   91509,   91609,   11116
91602,   1516,    90609,   90709,   1515,    11116,   91609,   91709,   11115
91702,   1515,    90709,   90809,   1514,    11115,   91709,   91809,   11114
91802,   1514,    90809,   90909,   1513,    11114,   91809,   91909,   11113
91001,   90101,   90102,   1534,    1537,    91101,   91102,   11134,   11137
91002,   90102,   90103,   1531,    1534,    91102,   91103,   11131,   11134
91003,   90103,   90104,   1528,    1531,    91103,   91104,   11128,   11131
91004,   90104,   90105,   1525,    1528,    91104,   91105,   11125,   11128
91005,   90105,   90106,   1524,    1525,    91105,   91106,   11124,   11125
91006,   90106,   90107,   1523,    1524,    91106,   91107,   11123,   11124
91007,   90107,   90108,   1522,    1523,    91107,   91108,   11122,   11123
91008,   90108,   90109,   1521,    1522,    91108,   91109,   11121,   11122
91901,   1505,    1506,    90902,   90901,   11105,   11106,   91902,   91901
**
*ELGEN, ELSET=INNER_BASE
91901,   8,        1,        1
**
```

```
**
***************
**TOWER_PT6**
***************
**
*NCOPY, old set=OUTER_BASE_O_U, newset=TOWER_PT6_UPPER, change number=1000, shift
0,0,2.500
0,0,0
**
*NFILL, NSET=TOWER_PT6_NODES
OUTER_BASE_O_U, TOWER_PT6_UPPER, 2, 500
TOWER_PT6_UPPER, TOWER_PT1_MID, 4, 2250
**
*ELEMENT, TYPE=S4R
2001, 2101, 2102, 2602, 2601
2025, 2125, 2128, 2628, 2625
2032, 2146, 2101, 2601, 2646
3001, 3101, 3102, 5352, 5351
3025, 3125, 3128, 5378, 5375
3032, 3146, 3101, 5351, 5396
**
*ELGEN, ELSET=TOWER_PT6
2001, 24, 1, 1, 2, 500, 100
2025, 7, 3, 1, 2, 500, 100
2032, 1, 1, 1, 2, 500, 100
3001, 24, 1, 1, 4, 2250, 100
3025, 7, 3, 1, 4, 2250, 100
3032, 1, 1, 1, 4, 2250, 100
**
******************
**TOWER_DETAIL**
******************
**
*NCOPY, old set=TOWER_PT3_UPPER, newset=TOWER_DETAIL_O_M1, change number=1000, shift
0,0,0.300
0,0,0
*NCOPY, old set=TOWER_DETAIL_O_M1, newset=TOWER_DETAIL_O_M2, change number=1000, shift
0,0,0.300
0,0,0
**
*NODE
15200,   0.0,      0.0,      10.6
15201,   0.95,     0.0,      10.6
15209,   0.0,      0.95,     10.6
15217,   -0.95,    0.0,      10.6
15225,   0.0,      -0.95,    10.6
**
*NGEN, LINE=C, NSET=TOWER_DETAIL_M_L
15201, 15209, 1, 15200
15209, 15217, 1, 15200
15217, 15225, 1, 15200
15225, 15201, 3, 15200
**
*NCOPY, old set=TOWER_DETAIL_M_L, newset=TOWER_DETAIL_M_M1, change number=1000, shift
0,0,0.300
0,0,0
*NCOPY, old set=TOWER_DETAIL_M_M1, newset=TOWER_DETAIL_M_M2, change number=1000, shift
0,0,0.300
0,0,0
*NCOPY, old set=TOWER_DETAIL_M_M2, newset=TOWER_DETAIL_M_U, change number=1000, shift
```

```
0,0,0.150
0,0,0
**
*NODE
15300,   0.0,      0.0,      11.1
15301,   0.45,     0.0,      11.1
15309,   0.0,      0.45,     11.1
15317,   -0.45,    0.0,      11.1
15325,   0.0,      -0.45,    11.1
**
*NGEN, LINE=C, NSET=TOWER_DETAIL_I_L
15301, 15309, 1, 15300
15309, 15317, 1, 15300
15317, 15325, 1, 15300
15325, 15301, 3, 15300
**
*NCOPY, old set=TOWER_DETAIL_I_L, newset=TOWER_DETAIL_I_M1, change number=1000, shift
0,0,0.08
0,0,0
*NCOPY, old set=TOWER_DETAIL_I_M1, newset=TOWER_DETAIL_I_M2, change number=1000, shift
0,0,0.08
0,0,0
*NCOPY, old set=TOWER_DETAIL_I_M2, newset=TOWER_DETAIL_I_U, change number=1000, shift
0,0,0.07
0,0,0
**
*NFILL, NSET=TOWER_DETAIL_NODES
TOWER_PT3_UPPER, TOWER_DETAIL_M_L, 2, 50
TOWER_DETAIL_O_M2, TOWER_DETAIL_M_M2, 2, 50
TOWER_DETAIL_O_M1, TOWER_DETAIL_M_M1, 2, 50
TOWER_DETAIL_M_L, TOWER_DETAIL_I_L, 2, 50
TOWER_DETAIL_M_M1, TOWER_DETAIL_I_M1, 2, 50
TOWER_DETAIL_M_M2, TOWER_DETAIL_I_M2, 2, 50
TOWER_DETAIL_M_U, TOWER_DETAIL_I_U, 2, 50
**
*ELEMENT, TYPE=C3D8R, ELSET=TOWER_DETAIL
15001, 15101, 15102, 15152, 15151, 16101, 16102, 16152, 16151
15025, 15125, 15128, 15178, 15175, 16125, 16128, 16178, 16175
15032, 15146, 15101, 15151, 15196, 16146, 16101, 16151, 16196
15051, 15151, 15152, 15202, 15201, 16151, 16152, 16202, 16201
15075, 15175, 15178, 15228, 15225, 16175, 16178, 16228, 16225
15082, 15196, 15151, 15201, 15246, 16196, 16151, 16201, 16246
15101, 15201, 15202, 15252, 15251, 16201, 16202, 16252, 16251
15125, 15225, 15228, 15278, 15275, 16225, 16228, 16278, 16275
15132, 15246, 15201, 15251, 15296, 16246, 16201, 16251, 16296
15151, 15251, 15252, 15302, 15301, 16251, 16252, 16302, 16301
15175, 15275, 15278, 15328, 15325, 16275, 16278, 16328, 16325
15182, 15296, 15251, 15301, 15346, 16296, 16251, 16301, 16346
**
*ELGEN, ELSET=TOWER_DETAIL
15001, 24, 1, 1, 2, 1000, 1000
15025, 7, 3, 1, 2, 1000, 1000
15032, 1, 1, 1, 2, 1000, 1000
15051, 24, 1, 1, 2, 1000, 1000
15075, 7, 3, 1, 2, 1000, 1000
15082, 1, 1, 1, 2, 1000, 1000
15101, 24, 1, 1, 3, 1000, 1000
15125, 7, 3, 1, 3, 1000, 1000
15132, 1, 1, 1, 3, 1000, 1000
15151, 24, 1, 1, 3, 1000, 1000
```

```
15175, 7, 3, 1, 3, 1000, 1000
15182, 1, 1, 1, 3, 1000, 1000
**
**
*NODE
92101,   0.290,    -0.290,   11.1
92105,   0,        -0.400,   11.1
92109,   -0.290,   -0.290,   11.1
92501,   0.400,    0,        11.1
92505,   0,        0,        11.1
92509,   -0.400,   0,        11.1
92901,   0.290,    0.290,    11.1
92905,   0,        0.400,    11.1
92909,   -0.290,   0.290,    11.1
**
*NGEN, NSET=TOWER_DETAIL_CENTER_lower
92101,   92105,   1
92105,   92109,   1
*NGEN, NSET=TOWER_DETAIL_CENTER_middle
92501,   92505,   1
92505,   92509,   1
*NGEN, NSET=TOWER_DETAIL_CENTER_upper
92901,   92905,   1
92905,   92909,   1
**
*NFILL, NSET=TOWER_DETAIL_CENTER_1
TOWER_DETAIL_CENTER_lower, TOWER_DETAIL_CENTER_middle, 4, 100
TOWER_DETAIL_CENTER_middle, TOWER_DETAIL_CENTER_upper, 4, 100
**
*NCOPY, old set=TOWER_DETAIL_CENTER_1, new set=TOWER_DETAIL_CENTER_2, change
number=1000, shift
0,         0,         0.080
*NCOPY, old set=TOWER_DETAIL_CENTER_2, new set=TOWER_DETAIL_CENTER_3, change
number=1000, shift
0,         0,         0.080
*NCOPY, old set=TOWER_DETAIL_CENTER_3, new set=TOWER_DETAIL_CENTER_4, change
number=1000, shift
0,         0,         0.070
**
*ELEMENT, TYPE=c3d8r, ELSET=TOWER_DETAIL
92101, 92101, 92201, 92202, 92102, 93101, 93201, 93202, 93102
**
*ELGEN, ELSET=TOWER_DETAIL
92101, 8, 100, 100, 8, 1, 1, 3, 1000, 1000
**
**
*ELEMENT, TYPE=c3d8r, ELSET=TOWER_DETAIL_CENTER_1
96101,   92101,   15337,   15340,   92201,   93101,   16337,   16340,   93201
96201,   92201,   15340,   15343,   92301,   93201,   16340,   16343,   93301
96301,   92301,   15343,   15346,   92401,   93301,   16343,   16346,   93401
96401,   92401,   15346,   15301,   92501,   93401,   16346,   16301,   93501
96501,   92501,   15301,   15302,   92601,   93501,   16301,   16302,   93601
96601,   92601,   15302,   15303,   92701,   93601,   16302,   16303,   93701
96701,   92701,   15303,   15304,   92801,   93701,   16303,   16304,   93801
96801,   92801,   15304,   15305,   92901,   93801,   16304,   16305,   93901
96102,   15321,   92109,   92209,   15320,   16321,   93109,   93209,   16320
96202,   15320,   92209,   92309,   15319,   16320,   93209,   93309,   16319
96302,   15319,   92309,   92409,   15318,   16319,   93309,   93409,   16318
96402,   15318,   92409,   92509,   15317,   16318,   93409,   93509,   16317
96502,   15317,   92509,   92609,   15316,   16317,   93509,   93609,   16316
```

```
96602,  15316,  92609,  92709,  15315,  16316,  93609,  93709,  16315
96702,  15315,  92709,  92809,  15314,  16315,  93709,  93809,  16314
96802,  15314,  92809,  92909,  15313,  16314,  93809,  93909,  16313
96001,  92101,  92102,  15334,  15337,  93101,  93102,  16334,  16337
96002,  92102,  92103,  15331,  15334,  93102,  93103,  16331,  16334
96003,  92103,  92104,  15328,  15331,  93103,  93104,  16328,  16331
96004,  92104,  92105,  15325,  15328,  93104,  93105,  16325,  16328
96005,  92105,  92106,  15324,  15325,  93105,  93106,  16324,  16325
96006,  92106,  92107,  15323,  15324,  93106,  93107,  16323,  16324
96007,  92107,  92108,  15322,  15323,  93107,  93108,  16322,  16323
96008,  92108,  92109,  15321,  15322,  93108,  93109,  16321,  16322
96901,  15305,  15306,  92902,  92901,  16305,  16306,  93902,  93901
**
*ELGEN, ELSET=TOWER_DETAIL_CENTER_1
96901,  8,      1,      1
**
*ELCOPY, ELEMENT SHIFT=1000, OLD SET=TOWER_DETAIL_CENTER_1, SHIFT NODES=1000,
NEW SET=TOWER_DETAIL_CENTER_2
*ELCOPY, ELEMENT SHIFT=1000, OLD SET=TOWER_DETAIL_CENTER_2, SHIFT NODES=1000,
NEW SET=TOWER_DETAIL_CENTER_3
**
*ELSET, ELSET=TOWER_DETAIL
TOWER_DETAIL_CENTER_1, TOWER_DETAIL_CENTER_2, TOWER_DETAIL_CENTER_3
**
***************
**TOWER_PT4**
***************
**
*NCOPY, old set=TOWER_DETAIL_M_U, newset=TOWER_PT4_M1, change number= 1000, shift
0,0,3.450
0,0,0
*NCOPY, old set=TOWER_PT4_M1, newset=TOWER_PT4_M2, change number= 1000, shift
0,0,3.050
0,0,0
*NCOPY, old set=TOWER_PT4_M2, newset=TOWER_PT4_U, change number=1000, shift
0,0,3.050
0,0,0
**
*NFILL, NSET=TOWER_PT4_NODES
TOWER_DETAIL_M_U, TOWER_PT4_M1, 4, 250
TOWER_PT4_M1, TOWER_PT4_M2, 4, 250
TOWER_PT4_M2, TOWER_PT4_U, 4, 250
**
*ELEMENT, TYPE=S4R
18001, 18201, 18202, 18452, 18451
18025, 18225, 18228, 18478, 18475
18032, 18246, 18201, 18451, 18496
**
*ELGEN, ELSET=TOWER_PT4
18001, 24, 1, 1, 12, 250, 250
18025, 7, 3, 1, 12, 250, 250
18032, 1, 1, 1, 12, 250, 250
**
*NODE
101101, 0.550,   -0.550,  14.8
101105, 0,       -0.800,  14.8
101109, -0.550,  -0.550,  14.8
101501, 0.800,   0,       14.8
101505, 0,       0,       14.8
101509, -0.800,  0,       14.8
```

```
101901, 0.550,   0.550,   14.8
101905, 0,       0.800,   14.8
101909, -0.550,  0.550,   14.8
**
*NGEN, NSET=TOWER_PT4_M1_lower
101101, 101105, 1
101105, 101109, 1
*NGEN, NSET=TOWER_PT4_M1_middle
101501, 101505, 1
101505, 101509, 1
*NGEN, NSET=TOWER_PT4_M1_upper
101901, 101905, 1
101905, 101909, 1
**
*NFILL, NSET=TOWER_PT4_M1_CENTER
TOWER_PT4_M1_lower, TOWER_PT4_M1_middle, 4, 100
TOWER_PT4_M1_middle, TOWER_PT4_M1_upper, 4, 100
**
*ELEMENT, TYPE=s4r
101101, 101101, 101201, 101202, 101102
**
*ELGEN, ELSET=TOWER_PT4_M1_CENTER
101101, 8, 100, 100, 8, 1, 1
**
*ELEMENT, TYPE=s4r, ELSET=TOWER_PT4_M1_CENTER
104101, 101101, 19237,  19240,  101201
104201, 101201, 19240,  19243,  101301
104301, 101301, 19243,  19246,  101401
104401, 101401, 19246,  19201,  101501
104501, 101501, 19201,  19202,  101601
104601, 101601, 19202,  19203,  101701
104701, 101701, 19203,  19204,  101801
104801, 101801, 19204,  19205,  101901
104102, 19221,  101109, 101209, 19220
104202, 19220,  101209, 101309, 19219
104302, 19219,  101309, 101409, 19218
104402, 19218,  101409, 101509, 19217
104502, 19217,  101509, 101609, 19216
104602, 19216,  101609, 101709, 19215
104702, 19215,  101709, 101809, 19214
104802, 19214,  101809, 101909, 19213
104001, 101101, 101102, 19234,  19237
104002, 101102, 101103, 19231,  19234
104003, 101103, 101104, 19228,  19231
104004, 101104, 101105, 19225,  19228
104005, 101105, 101106, 19224,  19225
104006, 101106, 101107, 19223,  19224
104007, 101107, 101108, 19222,  19223
104008, 101108, 101109, 19221,  19222
104901, 19205,  19206,  101902, 101901
**
*ELGEN, ELSET=TOWER_PT4_M1_CENTER
104901, 8,       1,       1
**
*NCOPY, old set=TOWER_PT4_M1_CENTER, new set=TOWER_PT4_M2_CENTER, change number=1000,
shift
0,       0,       3.050
**
*ELCOPY, ELEMENT SHIFT=1000, OLD SET=TOWER_PT4_M1_CENTER, SHIFT NODES=1000, NEW
SET=TOWER_PT4_M2_CENTER
```

```
**
*NCOPY, old set=TOWER_PT4_M2_CENTER, new set=TOWER_PT4_U_CENTER, change number=1000,
shift
0,          0,          3.050
**
*ELCOPY, ELEMENT SHIFT=1000, OLD SET=TOWER_PT4_M2_CENTER, SHIFT NODES=1000, NEW
SET=TOWER_PT4_U_CENTER
**
*NODE
21500,   0.0,       0.0,       20.9
21501,   1.75,      0.0,       20.9
21509,   0.0,       1.75,      20.9
21517,   -1.75,     0.0,       20.9
21525,   0.0,       -1.75,     20.9
**
*NGEN, LINE=C, NSET=TOWER_PT4_U_CENTER_1
21501, 21509, 1, 21500
21509, 21517, 1, 21500
21517, 21525, 1, 21500
21525, 21501, 3, 21500
**
*NFILL, NSET=TOWER_PT4_U_CENTER
TOWER_PT4_U, TOWER_PT4_U_CENTER_1, 3, 100
**
*ELEMENT, TYPE=s4r
21201, 21201, 21202, 21302, 21301
21225, 21225, 21228, 21328, 21325
21232, 21246, 21201, 21301, 21346
21401, 21401, 21402, 21502, 21501
21425, 21425, 21428, 21528, 21525
21432, 21446, 21401, 21501, 21546
**
*ELGEN, ELSET=TOWER_PT4_U_CENTER
21201, 24, 1, 1, 3, 100, 100
21225, 7, 3, 1, 3, 100, 100
21232, 1, 1, 1, 3, 100, 100
**
**************************************
**NODE AND ELEMENT SET DEFINITIONS**
**************************************
**
*NSET, NSET=LOAD_POA
13617
**
*NSET, NSET=WATERLEVEL
14117
**
*NSET, NSET=BASE_BOUNDARY
OUTER_BASE_I_L, OUTER_BASE_BOTTOM, INNER_BASE_1
**
*ELSET, ELSET=ConcrFilled
TOWER_PT1, TOWER_PT2
**
************************
**SECTION DEFINITIONS**
************************
**
*SOLID SECTION, MATERIAL=INNER_BASE, ELSET=INNER_BASE
*SOLID SECTION, MATERIAL=OUTER_BASE, ELSET=OUTER_BASE
*SOLID SECTION, MATERIAL=CONCRETE, ELSET=TOWER_DETAIL
```

```
*SHELL SECTION, MATERIAL=CONCRETEPART1, ELSET=TOWER_PT1, OFFSET=SPOS
0.5, 5
*SHELL SECTION, MATERIAL=CONCRETEPART3, ELSET=TOWER_PT3, OFFSET=SPOS
0.5, 5
*SHELL SECTION, MATERIAL=CONCRETE_LOADSECTION, ELSET=TOWER_PT2, OFFSET=SPOS
0.5, 5
*SHELL SECTION, MATERIAL=CONCRETEPART4, ELSET=TOWER_PT4, OFFSET=SPOS
0.2, 5
*SHELL SECTION, MATERIAL=CONCRETE, ELSET=TOWER_PT4_M1_CENTER, OFFSET=SPOS
0.2, 5
*SHELL SECTION, MATERIAL=CONCRETE, ELSET=TOWER_PT4_M2_CENTER, OFFSET=SPOS
0.15, 5
*SHELL SECTION, MATERIAL=CONCRETE, ELSET=TOWER_PT4_U_CENTER, OFFSET=SPOS
0.2, 5
*SHELL SECTION, MATERIAL=CONCRETEPART6, ELSET=TOWER_PT6, OFFSET=SPOS
0.4, 5
*END PART
**
**************
**ASSEMBLY**
**************
**
*ASSEMBLY, NAME=LIGHTHOUSE
**
*INSTANCE, NAME=LIGHTHOUSE, PART=LIGHTHOUSE
            0.0,        0.0,        0.0
*END INSTANCE
**
*END ASSEMBLY
**
***************
**MATERIALS**
***************
**
*Material, name=INNER_BASE
*Density
2400.,
*Elastic
 3.4e+10, 0.15
*Material, name=OUTER_BASE
*Density
15364.,
*Elastic
 3.4e+10, 0.15
*Material, name=Concrete
*Density
2400.,
*Elastic
 3.4e+10, 0.15
*Material, name=ConcretePart1
*Density
5172.,
*Elastic
 3.4e+10, 0.15
*Material, name=Concrete_loadsection
*Density
5172.,
*Elastic
 3.4e10, 0.15
*Material, name=ConcretePart3
```

```
*Density
2193.,
*Elastic
 3.4e+10, 0.15
*Material, name=ConcretePart4
*Density
2274.,
*Elastic
 3.4e+10, 0.15
*Material, name=ConcretePart6
*Density
1880.,
*Elastic
 3.4e+10, 0.15
*Material, name=SEABED_LAYER1
*Elastic
 8e+07, 0.3
*Material, name=SEABED_LAYER2
*Elastic
 1e+08, 0.3
*Material, name=SEABED_LAYER3
*Elastic
 1.2e+08, 0.3
*Material, name=SEABED_LAYER4
*Elastic
 1.4e+08, 0.3
*Material, name=SEABED_LAYER5
*Elastic
 1.6e+08, 0.3
**
```